Identifikacija motornih proteina u premosnom vlaknu mitotskog diobenog vretena

Risteski, Patrik

UNIVERSITY OF ZAGREB
FACULTY OF SCIENCE
DEPARTMENT OF BIOLOGY

Patrik Risteski

IDENTIFICATION OF MOTOR PROTEINS IN THE BRIDGING FIBER OF THE MITOTIC SPINDLE

Graduation thesis

Zagreb, 2017.

This thesis was done in Laboratory of Cell Biophysics, Division of Molecular Biology, Ruđer Bošković Institute, under the mentorship of Prof. Dr. Iva Tolić (Division of Molecular Biology, Ruđer Bošković Institute, 10000 Zagreb, Croatia), and the co-mentorship of Assoc. Prof. Dr. Biljana Balen (Department of Molecular Biology, Faculty of Science, University of Zagreb, 10000 Zagreb, Croatia). Work in this thesis was supported by European Research Council (ERC) project entitled NewSpindleForce (GA Number 647077).

Acknowledgements

First of all, I would like to give special thanks to my mentor, Iva Tolić. I am very grateful for the opportunities you have given me and for inspiring me to pursue a cell biologist career. Thank you for your guidance and advices, and for all the knowledge and skills, from thoroughness to critical evaluation, I have gained under your mentorship. Thank you for allowing me to be part of your group. It has been an honor.

Furthermore, thanks are due to Biljana Balen, my co-mentor, for interest in this thesis, discussions and commentary.

Next, I would like to thank my dear filmophile, foodie, and Star Wars enthusiast, Ivana, who has taught me all the tricks and tips for Adobe Illustrator. Thank you for all your help, support, and being a friend during my time in the group. I appreciate it.

Thanks are due to Sonja for her help with the cell culture. To my fellow lab-mates, thank you for all the excitement and fun you bring to the lab, and energize each other to continue the research. Their names are as follows: Ana, Barbara, Bruno, Jelena, Juraj, Kruno, Luka, Mihaela, and Renata. I am also thankful to Nenad Pavin and all members of Pavin group for all discussions and commentary from the theoretical physics perspective.

Moreover, I would like to thank my family for their support over the years and for allowing me to realize my own potential. I need to further thank all my friends for being beside me over the years. At last, I am thankful to my better half, who has never stopped reminding me that I am able to handle anything I set my mind to. Your support and encouragement was worth more than I can express.

TEMELJNA DOKUMENTACIJSKA KARTICA

Sveučilište u Zagrebu
Prirodoslovno-matematički fakultet
Biološki odsjek Diplomski rad

Identifikacija motornih proteina u premosnom vlaknu mitotskog diobenog vretena

Patrik Risteski
Rooseveltov trg 6, 10000 Zagreb, Hrvatska

Na početku mitoze, stanica konstruira diobeno vreteno, dinamičnu strukturu odgovornu za preciznu segregaciju repliciranog genoma između stanica kćeri. Ova jedinstvena citoskeletna struktura sastavljena je od kromosoma, mikrotubula i proteina povezanih s mikrotubulima. Nedavna istraživanja su započela s otkrivanjem nove grupe mikrotubula, nazvanih mikrotubuli premosnice, koji premošćuju regiju između sestrinskih kinetohora i pritom tvore premosno vlakno, lateralno povezano sa sestrinskim k-vlaknima. U ovom radu, identificiran je položaj motornih proteina povezanih s mikrotubulima u mitotskom diobenom vretenu stanica HeLa u odnosu na pozicije premosnih vlakana. Protein MKLP1, motor kinezin-6, pronađen je kako obogaćuje centralni dio diobenog vretena na pozicijama premosnih vlakana. Prekomjerna ekspresija proteina PRC1, antiparalelnog veznika koji je potvrđen u premosnom vlaknu, pokazala je korelaciju između lokalizacije proteina MKLP1 i premosnih preklapajućih regija označenih s proteinom PRC1. Nadalje, utišavanje Kif4A, poznatog veznog partnera proteina PRC1, uzrokuje elongaciju preklapajućih regija premosnih vlakana.

(60 stranica, 33 slike, 82 literaturna navoda, jezik izvornika: engleski)

Ključne riječi: motorni protein, kinezin, dinein, PRC1, mikrotubuli premosnice, mitoza

Voditelj: dr. sc. Iva Tolić, prof.
Suvoditelj: dr. sc. Biljana Balen, izv. prof.

Ocjenitelji:
1. dr. sc. Biljana Balen, izv. prof.
2. dr. sc. Martina Šeruga Musić, izv. prof.
3. dr. sc. Duje Lisičić, doc.

Zamjena: dr. sc. Maja Matulić, izv. prof.

BASIC DOCUMENTATION CARD

University of Zagreb
Faculty of Science
Department of Biology

Graduation thesis

Identification of motor proteins in the bridging fiber of the mitotic spindle

Patrik Risteski
Rooseveltov trg 6, 10000 Zagreb, Croatia

At the onset of mitosis, cell constructs a spindle, a dynamic structure responsible for precise segregation of replicated genome between daughter cells. This unique cytoskeletal apparatus is made of chromosomes, microtubules and microtubule-associated proteins. Recent studies have begun to uncover a new class of microtubules, termed bridging microtubules, that span the region between sister kinetochores, whilst forming the bridging fiber that laterally connects sister k-fibers. In this thesis, I have identified localization of motor microtubule-associated proteins in the mitotic spindle of HeLa cells with respect to the bridging fiber positions. MKLP1, a kinesin-6 motor, was observed to enrich the central part of the spindle at the positions of the bridging fibers. Overexpression of PRC1, an anti-parallel cross-linker, which is confirmed in the bridging fibers, shows correlation of MKLP1 localization with PRC1-labeled bridging overlaps. Additionally, silencing of Kif4A, a major binding partner of PRC1, elongates overlap regions of the bridging fibers.

(60 pages, 33 figures, 82 references, original in English)

Keywords: motor protein, kinesin, dynein, PRC1, bridging microtubules, mitosis

Supervisor: Dr. Iva Tolić, Prof.
Co-supervisor: Dr. Biljana Balen, Assoc. Prof.

Reviewers:
1. Dr. Biljana Balen, Assoc. Prof.
2. Dr. Martina Šeruga Musić, Assoc. Prof.
3. Dr. Duje Lisičić, Asst. Prof.

Substitute: Dr. Maja Matulić, Assoc. Prof.

Table of Contents

1. Introduction

Cell division is a core process of life that enables segregation of genetic material. It is therefore not surprising that defects in the cell division are associated with a various range of diseases. In all eukaryotes during cell division, a microtubule-based micro-apparatus known as the spindle is responsible for faithful segregation of genetic material into two daughter cells. Assembly of the bipolar spindle, together with non-erroneous spindle function, requires regulation of microtubule dynamics and the activity of various microtubule-associated motor and non-motor proteins.

Recent work has begun to uncover the mechanism that balances the tension between sister kinetochores and helps the spindle to obtain a rounded shape (Kajtez et al., 2016). The structure that underpins this balance is a bridging fiber, a bundle consisting of a new subset of non-kinetochore microtubules that interdigitate at the central part of the spindle, while spanning the region between sister kinetochore fibers (k-fibers) and associating with them into a single mechanical object (Kajtez et al., 2016). This overlap bundle, made of antiparallel microtubules, is cross-linked with non-motor protein, protein regulator of cytokinesis 1 (PRC1). It was shown that virtually all PRC1-labeled antiparallel bundles associate with sister kinetochores and sister k-fibers, suggesting that all PRC1-labeled bundles are bridging fibers (Polak et al., 2017). However, localization of motor proteins within the bridging fibers that generate forces to separate chromosomes or act as a mechanical support for the k-fibers is yet to be investigated.

The goal of this thesis was to identify localization of motor proteins in the spindle with respect to the bridging fiber positions. HeLa cells immunostained for kinesin-4 (Kif4A) or stably expressing kinesin-5 (Eg5), kinesin-6 (MKLP1), kinesin-8 (Kif18A), kinesin-13 (MCAK), and cytoplasmic dynein 1 (DN1CH1) were used together with staining of microtubules by SiR-tubulin dye. Due to localization of PRC1 in the bridging fibers, overexpression of this passive cross-linker with mCherry-PRC1 plasmid was used to investigate effects on the relocalization of motor proteins. Additionally, Kif4A is a major binding partner of PRC1. Thus, silencing of Kif4A with Kif4A small interfering RNA (siRNA) was used to investigate effects on the PRC1-labeled bridging fibers.

1.1. The eukaryotic cell cycle

Cell division, essentially a duplication process, produces two genetically identical cells from a single one. In order to divide into two daughter cells, a cell must undergo several crucial events that precede the cell division, i.e. cell growth, DNA replication and physical distribution of the duplicated genetic material. Cells undergo these coordinated events in organized, discrete phases that make up the cell cycle (**Figure 1**) (Alberts et al., 2007). On average, eukaryotic cell cycle lasts for 24 hours. The major phases of the cell cycle are synthesis (S) phase, in which genetic material duplication occurs and mitotic (M) phase, in which duplicated genetic material is divided into daughter cells. Together with S phase, gap (G_1 and G_2) phases make interphase. G phases, marked with the cell growth, separate M phase from S phase and *vice versa*. M phase consists of mitosis, which involves the division and duplication of the cell's nucleus, and cytokinesis, which involves cytoplasmic division. M phase lasts only about an hour, so approximately 95% of the time cell spends in the interphase.

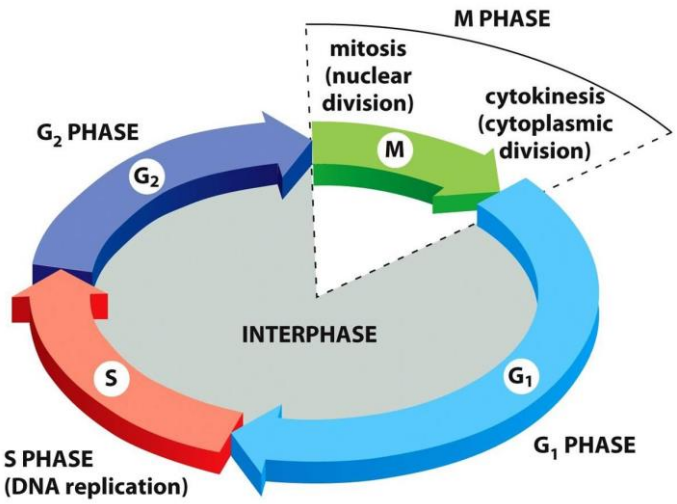

Figure 1. The phases of the cell cycle. Interphase consists of three phases: DNA replication is limited to S phase, G_1 is the gap between M phase and S phase, while G_2 is the gap between S phase and M phase. In M phase, first the nucleus and then the cytoplasm divide (Alberts et al., 2007).

1.2. Regulation of the cell cycle

Conserved regulatory apparatus coordinates various events in the cell cycle. Coordination is accomplished by series of control points that regulate progression through different phases. There are three clearly defined control points or checkpoints that occur in the cell cycle – the G_1 checkpoint at the G_1/S transition, the S checkpoint during S phase, the G_2 checkpoint at the G_2/M transition and the spindle assembly checkpoint (SAC) at the transition from metaphase to anaphase (**Figure 2**) (Cooper and Hausman, 2003). Chronologically first checkpoint is passed if cell's environment is favorable and cell's DNA quality is good. The S checkpoint controls the integrity of DNA. The G_2 checkpoint blocks the initiation of mitosis until DNA replication is completed and if necessary repaired. The following checkpoint, the SAC checkpoint allows segregation of chromosomes when all chromosomes are properly aligned and attached to the mitotic spindle.

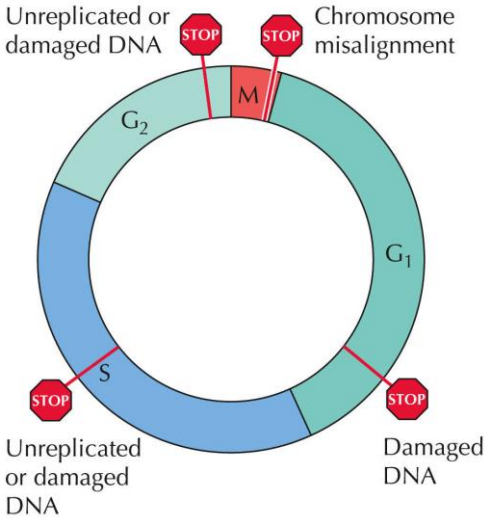

Figure 2. The cell cycle checkpoints. Throughout the cell cycle, a cell must pass several checkpoints to ensure non-erroneous cell division. During interphase, cell is tested for quality of DNA at G_1, S, and G_2 checkpoints and DNA replication at S and G_2 checkpoints. To proceed with cell division, chromosome misalignment is tested at the SAC checkpoint in M phase (Cooper and Hausman, 2003).

Cell cycle is regulated via a family of protein kinases named cyclin-dependent kinases (CDKs), by their activation and inactivation. The four major mechanisms of CDK regulation are cyclin binding, CDK-activating kinase (CAK) phosphorylation, regulatory inhibitory phosphorylation, and binding of CDK inhibitors (CKIs) (Alberts et al., 2007). Each cyclin is associated with a particular phase or transition – G_1 cyclins, G/S cyclins, S cyclins, and M cyclins. Cyclins bind to inactive CDKs making them functional enzymes and allowing them to phosphorylate targeted proteins. CAK activates the CDK-cyclin via phosphorylation. Contrary, specific nuclear kinases inhibit CDK by preventing activation of the CDK-cyclin complex. CKI proteins bind to CDK-cyclin complexes and block their activity, thus preventing cell to pass the checkpoints (Alberts et al., 2007).

1.3. Mitotic phase

As the most eventful phase of the cell cycle, M phase involves a major rearrangement of virtually all cell components. Amid nuclear division, the chromatin condenses into chromosomes, the nuclear envelope breaks down and interphase cytoskeleton network reorganizes into the mitotic spindle that separates chromosomes to opposing poles. Conventionally, mitosis consists of five stages – prophase, prometaphase, metaphase, anaphase and telophase (**Figure 3**) (Cooper and Hausman, 2003).

As the cell passes G_2 checkpoint, prophase starts. Prophase is evident by chromosomes condensation, an event required for their separation during later stages of mitosis. During prophase, the chromosomes are still confined within the intact nuclear envelope. The chromosomes contain centromere regions where kinetochores assemble. Duplicated centrosomes, as the organizing centers of microtubules, begin to separate towards opposite poles of the cell and construct the mitotic spindle during the late prophase.

Nuclear envelope breakdown into small vesicles marks the onset of prometaphase. Without nuclear envelope, the mitotic spindle is able to attach now matured kinetochores, protein complexes built on centromeres of chromosomes (Musacchio and Desai, 2017). Having captured kinetochores, microtubules start exerting forces on the chromosomes and move them.

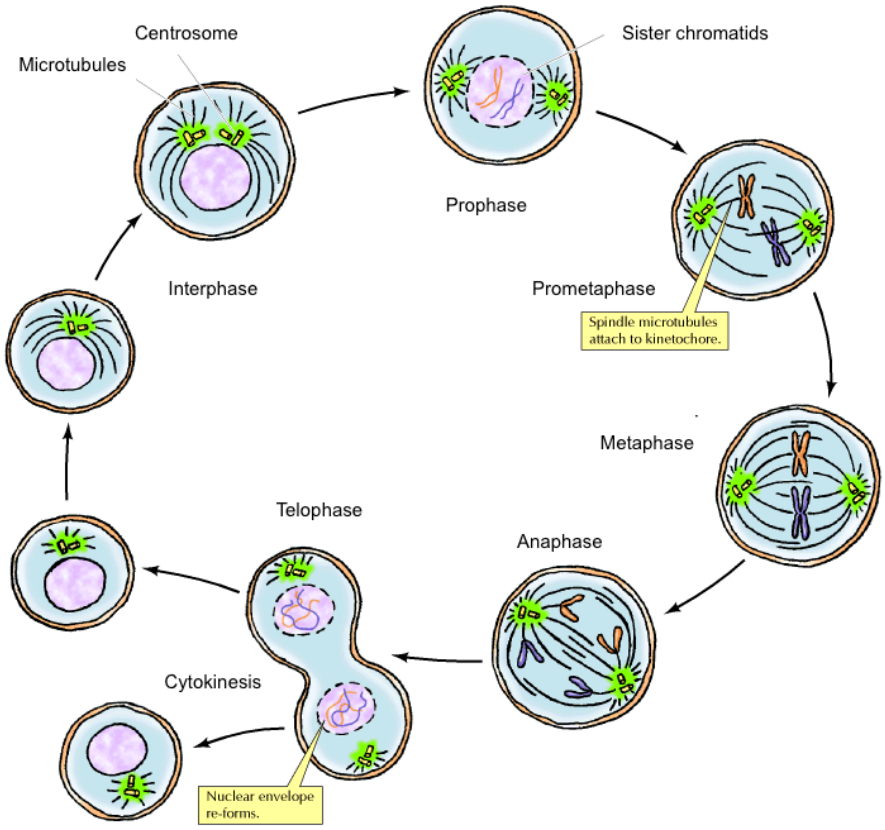

Figure 3. The stages of mitosis. Mitosis starts with prophase when centrosomes separate and chromosomes condense. During prometaphase, microtubules incorporate chromosomes via kinetochores into a bipolar spindle. Metaphase is evident by the chromosome alignment in the metaphase plate. In anaphase, sister chromatids start to separate to the opposite poles of the spindle. Mitosis finishes with telophase when chromosomes start to decondese and the nuclei are re-formed. During cytokinesis cells divide into two daughter cells (Cooper and Hausman, 2003).

Metaphase is evident by the congression of chromosomes at the central part of the mitotic spindle, i.e. at the equatorial plane. When chromosomes get properly aligned, anaphase starts. During anaphase, sister chromatids separate as they are moved toward the opposite spindle poles. Anaphase can be divided into two distinct phases – anaphase A and anaphase B. In anaphase A, chromosomes move towards the pole, while in anaphase B, spindle poles separate by elongation of non-kinetochore microtubules (Scholey et al., 2016).

At the final stage of mitosis, telophase, the sister chromatids reach the opposite poles and nuclear envelope around opposite groups of chromosomes starts to form. As the nuclear envelopes re-form, the chromosomes begin to decondense. The cell cytoplasm separates after chromosome segregation and reforming of nuclei, thereby leading to cell division in the final stage of M phase – cytokinesis.

1.4. Cytoskeleton and microtubules

Unique to eukaryotic cells, cytoskeleton is a complex three-dimensional network, made of interlinking filamentous proteins, that helps cell to maintain shape and internal organization, and provide mechanical support that ensures integral functions like movement and cell division. Cytoskeleton consists of three major classes of elements that differ in function, length, diameter, and protein composition – microtubules, actin filaments and intermediate filaments (Alberts et al., 2007).
Microtubules are stiff cylindrical tubes approximately 25 nm in diameter, made of globular tubulin subunits (**Figure 4**) (Alberts et al., 2007). Tubulin is a heterodimer, which consists of α- and β-tubulin monomers that both weight 55 kDa and have considerable homology. Microtubules assemble by end-to-end polymerization of αβ-tubulin dimers into linear protofilamets. Generally, a single microtubule is formed by the lateral association of thirteen protofilaments, which can then be extended by the addition of more αβ-tubulin dimers.

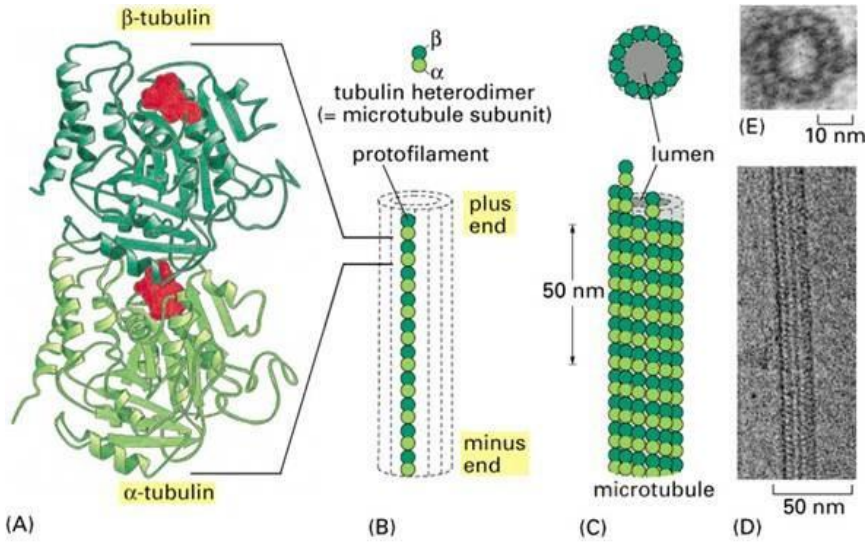

Figure 4. The structure of a microtubule and its subunits. (A) The building block of each protofilament is a tubulin heterodimer made of α- and β-monomer bound to one GTP molecule (red). (B) End-to-end assembly of αβ-heterodimers constructs a protofilament. (C) Protofilaments laterally associate into a stiff hollow tube, a microtubule. (D) Segment of a microtubule viewed in an electron microscope. (E) Electron micrograph of a cross section of a microtubule showing a ring of thirteen protofilaments (Alberts et al., 2007).

Microtubules have a well-defined polarity that is crucial for their biological roles. As a result of tubulin end-to-end polymerization, one end in a protofilament will have the α-subunit exposed while the other will have the β-subunit exposed. Since protofilaments associate laterally to one another with the same polarity, microtubule ends with α-subunits exposed are named minus (-) ends, while microtubule ends with the β-subunits exposed are named plus (+) ends, respectively (Alberts et al., 2007).
Tubulin subunits are bound to the energy carrier, guanosine triphosphate (GTP). After incorporation into a microtubule, GTP is hydrolyzed into guanosine diphosphate (GDP). Unlike GTP-tubulin, GDP-tubulin undergoes depolymerization. GDP-tubulin at the one end of a microtubule will tend to disassemble. Since microtubule polymerizes by adding tubulin in the GTP-bound state, a cap of GTP-tubulin exists at the other end of the microtubule, protecting it from disassembly. If hydrolysis progresses to the end of the microtubule, microtubule undergoes a rapid depolymerization and shrinkage. Switching from growth to shrinkage is termed

"catastrophe". When addition of GTP-tubulin starts again at the end of a microtubule, microtubule is rescued from the shrinking, thus termed "rescue". This dynamic behavior is referred to as dynamic instability (**Figure 5**) (Alberts et al., 2007).

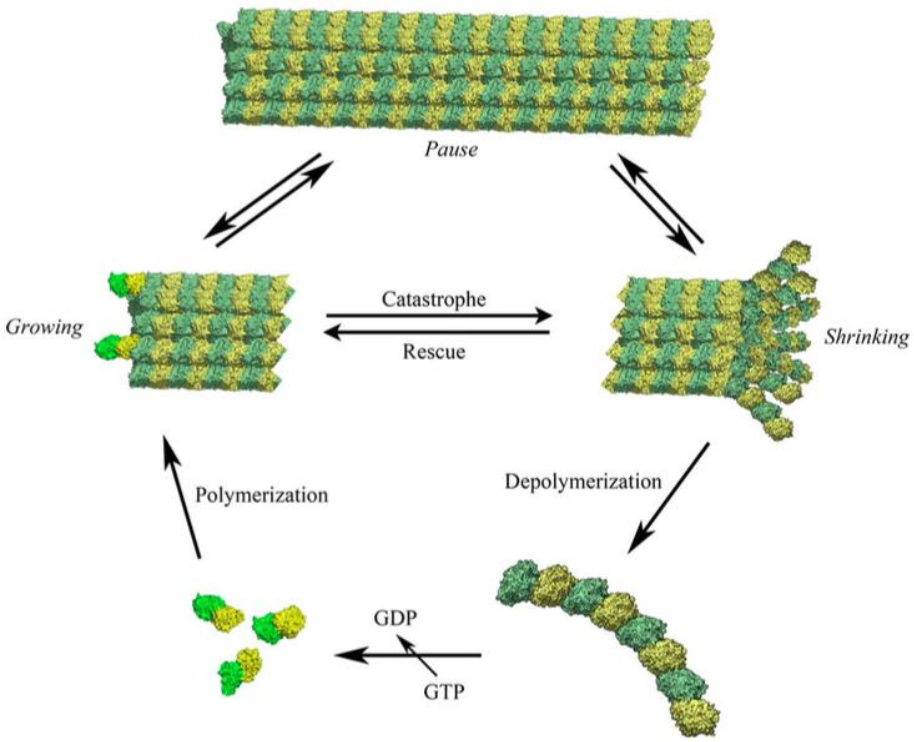

Figure 5. Dynamic instability of microtubules. Microtubules switch between growing and shrinking events. A depolymerizing microtubule is indicated by the peeling arrays of spiral protofilaments at its end. A shrinking event is finished by regeneration of tubulin heterodimers. The exchange of a guanine nucleotide on the tubulin heterodimer begins a new cycle. The protofilaments polymerize to generate a metastable intermediate structure. α- and β-tubulin subunits are shown in yellow and green, respectively (Marchetti et al., 2016).

1.5. The mitotic spindle

Centrosome, essentially the main microtubule organizing center of the animal cell, is composed of two orthogonal centrioles enclosed by an amorphous mass, which contains proteins responsible for microtubule nucleation. After duplication in interphase, centrosomes with emanating microtubules start to assemble a bipolar spindle at the onset of mitosis. Even though the pathway of spindle assembly differs among the cell types, all spindles share common structural features (Waters and Salmon, 1997).

The spindle is a dynamic and complex micro-apparatus made of microtubules and the associated proteins (Pavin and Tolić, 2016). Microtubules inside the spindle attach to centromere regions of chromosomes via multi-protein complexes termed kinetochores (Cheeseman and Desai, 2008; Musacchio and Desai, 2017). Microtubules attached to kinetochores generate forces on them. Beside chromosome separation, forces are also responsible for chromosome congression to the metaphase plate and silencing of the SAC (Nezi and Musacchio, 2009).

Microtubules within the mitotic spindle can be divided into two groups – kinetochore microtubules that end at the kinetochores and non-kinetochore microtubules that do not (**Figure 6**). Emanating from spindle poles, kinetochore microtubules with their plus ends attach to the kinetochores and form parallel bundles, known as kinetochore fibers (k-fibers). Images acquired by the electron microscopy showed that the k-fiber in a human cell consists of 12-22 parallel microtubules (Wendell et al., 1993; McEwen et al., 2001). Non-kinetochore microtubules can be divided into polar, interpolar and astral microtubules (**Figure 6**). Astral microtubules emanate from spindle poles and grow toward the cell cortex. Polar microtubules emanate from spindle poles and with their free plus ends grow toward the center of the spindle. Interpolar microtubules emerge when polar microtubules, from opposite poles, interact in the central part of the spindle, thereby forming antiparallel overlaps. Interpolar microtubules are also referred to as overlap microtubules (Alberts et al., 2007).

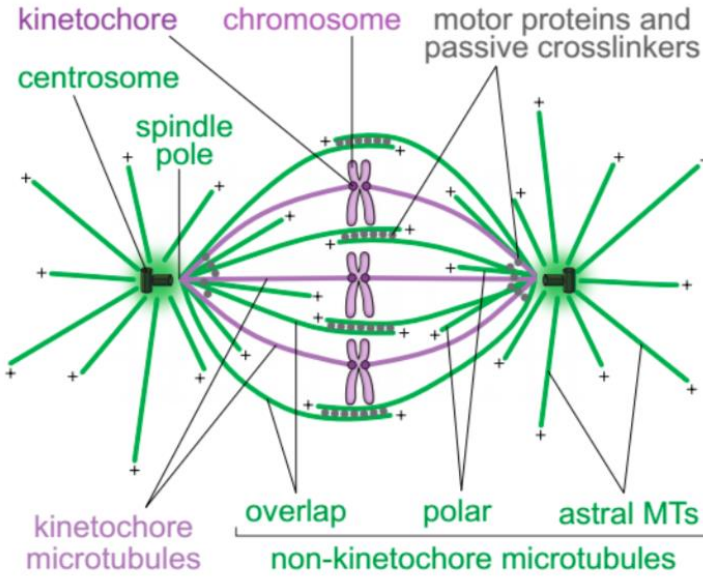

Figure 6. Classes of microtubules in the mitotic spindle. Microtubules are dominantly nucleated at the centrosome, which serves as the spindle pole. Chromosomes are attached to kinetochore microtubules via kinetochores. Non-kinetochore microtubules are polar microtubules that grow toward the spindle center, overlap microtubules that interdigitate at the spindle center, and astral microtubules that grow toward the cell cortex (Tolić, 2017).

1.6. Bridging microtubules

During mitosis, the main role of the mitotic spindle is to generate forces that align the chromosomes at the equatorial plane and later pull them apart toward the opposite spindle poles. It is thought that forces exerted on kinetochores are mainly generated by the k-fibers that interact with them. On the other hand, interpolar microtubules do not interact with kinetochores and their interactions with k-fibers are weak and solely exist near the spindle poles (**Figures 6** and **7A**). Hence, the classical view of the mitotic spindle places the origin of the forces mainly on the k-fibers, under which conditions the k-fibers are expected to be straight (Simunić and Tolić, 2016).

However, in various species the k-fibers are rounded rather than straight (Tolić and Pavin, 2016). Using electron microscopy, interpolar microtubules have been observed in the proximity of k-fibers and between sister kinetochores in the metaphase of

various organisms (Jensen, 1982; McDonald et al., 1992; Ohi et al., 2003). Recent studies have shown that a bundle of overlap microtubules, named bridging fiber, balances the tension between sister kinetochores and supports a rounded shape of the spindle (**Figure 7B**) (Kajtez et al., 2016; Milas and Tolić, 2016). Notably, the bridging fibers are formed of antiparallel microtubules suggesting that bridging fibers are a subgroup of interpolar microtubules. By using laser-cutting experiments, it was shown that these microtubules bridge the region between sister kinetochores and connect both sister k-fibres and kinetochores into a single mechanical object able to withstand physical perturbations (Kajtez et al., 2016). Additionally, presence of the bridging microtubules was observed by electron microscopy (Nixon et al., 2017).

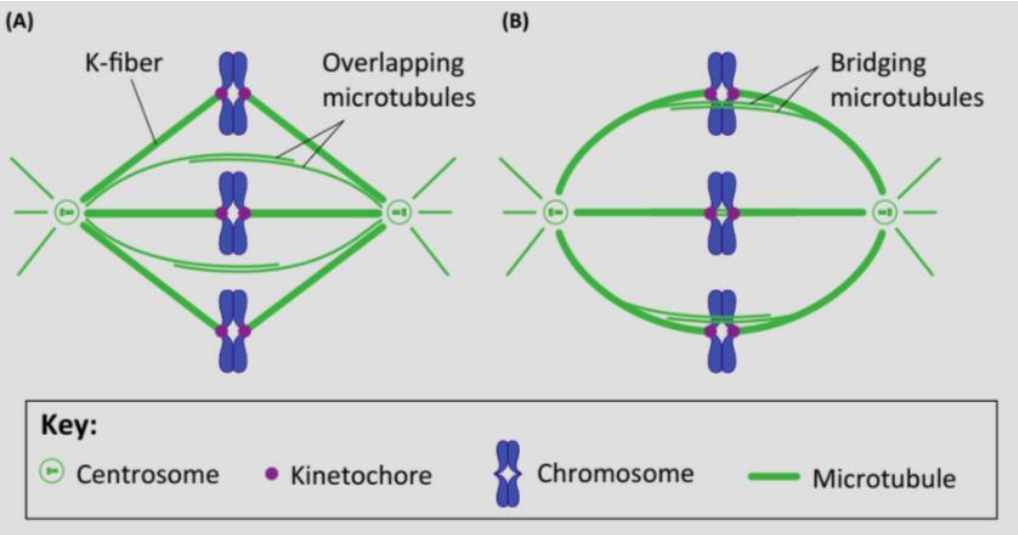

Figure 7. The classical and the new view of the mitotic spindle. (A) In the classical view of the mitotic spindle, the tensed k-fibers are expected to be straight. Overlap microtubules do not interact with k-fibers. (B) In the new view of the mitotic spindle, k-fibers laterally interact with overlapping microtubules along their length. Sister k-fibers together with their bridging fiber are curved, which represents the shape of the spindle observed under the microscope (Simunić and Tolić, 2017).

1.7. Proteins of the mitotic spindle

Even though the most abundant components of the spindle are microtubules, various proteins need to be involved so that the spindle ensures faithful chromosome segregation. Many microtubule-associated proteins (MAPs) help to organize the spindle and help the spindle to function properly. Several classes can be distinguished accordingly – proteins that promote and stabilize microtubule polymerization, proteins that destabilize or severe microtubules, proteins that function as linkers between various structures, and proteins with motility-related functions (Maiato et al., 2004).

Non-motor MAPs are non-motile proteins that have diverse contribution to mitotic spindle organization, including the nucleation and organization of microtubules, influence on motor function, and regulation of the cell cycle control (Manning and Compton, 2008). Contrary, motor proteins utilize the chemical energy released by the hydrolysis of adenosine triphosphate (ATP) in order to perform active directional movement along microtubules through interaction with tubulin. There are two basic classes of microtubule motors – plus-end motors, which directionally move toward the plus ends of microtubules and minus-end motors, which directionally move toward the minus ends, respectively. Conventionally, plus-end motors are namely kinesins, whereas minus-end motors are dyneins (Alberts et al., 2007). In addition, non-motor MAPs can interact with motor proteins and in some circumstances directly influence their function (Merdes et al., 2000). Among all MAPs, a passive cross-linking protein and several motor proteins have a specific focus in this thesis and therefore will be studied thoroughly.

1.8. Protein regulator of cytokinesis 1

Protein regulator of cytokinesis 1 (PRC1) is a highly conserved non-motor MAP that acts as a passive cross-linker of the antiparallel microtubules (Kapitein et al. 2008; Bieling et al., 2010; Subramanian et al., 2013). Beside *in vitro* experiments, PRC1 was shown to localize to the antiparallel microtubules of the spindle midzone

(Pellman et al., 1995; Jiang et al., 1998; Mollinari et al., 2002; Kurasawa et al., 2004; Zhu and Jiang, 2005) where its role in cytokinesis is integral (Zhu et al., 2006).

Its affinity to bind to microtubules is regulated by phosphorylation and dephosphorylation events. When phosphorylated, PRC1 is able to bind to microtubules, yet unable to cross-link them. Following dephosphorylation, PRC1 bundles neighboring microtubules and stabilizes formed antiparallel overlaps (Mollinari et al., 2002; Neef et al., 2007; Subramanian et al., 2010).

Even though mandatory for its microtubule-bundling activity, which is important for the assembly of the spindle's midzone, little was known of PRC1-crosslinked antiparallel microtubules beyond anaphase (Mollinari et al., 2002; Kurasawa et al., 2004). Recently, PRC1 was observed to localize to the central part of the metaphase spindle, in the bridging fibers (**Figure 8A**) (Kajtez et al., 2016; Polak et al., 2017). Interestingly, it was shown that bridging fibers, indicated by PRC1-labeled bundles, and kinetochore pairs show one-to-one relationship throughout the spindle (**Figure 8B**) (Polak et al., 2017).

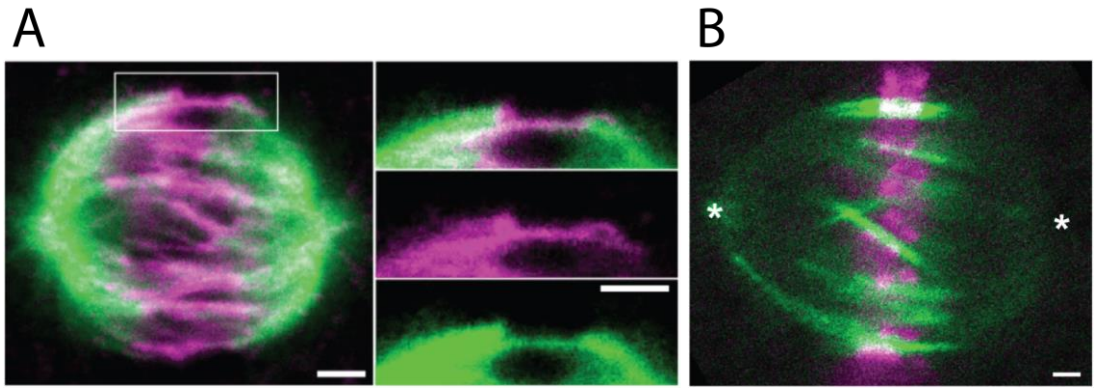

Figure 8. PRC1 localizes to central part of the metaphase spindle. (A) Hela cell stably expressing tubulin-GFP (green) and immunostained for endogenous PRC1 (Alexa Fluor-555, magenta). Enlargements of the boxed region (top: merge, middle: GFP, bottom: Alexa Fluor-555) show the endogenous PRC1 (magenta) localization to the bridging fiber (green). (B) HeLa cell stably expressing PRC1-GFP (green) and transiently mRFP-CENP-B (magenta), which indicates kinetochores. PRC1 binds to the antiparallel overlap zones and indicates bridging fibers (Polak et al., 2017).

1.9. Kinesin-5

Antiparallel regions of interpolar microtubules contain motor proteins that can contribute to antiparallel microtubule sliding. In most eukaryotic cells, kinesin-5 is thought to have a great importance in relative sliding and sorting of microtubules of the mitotic spindle (Kashina et al., 1996; Kapoor, 2017). As a homotetrameric plus-end directed motor protein, kinesin-5 can both slide apart antiparallel microtubules and cross-link parallel ones without sliding them relative to each other (**Figure 9**) (Kapitein et al. 2005, Shimamoto et al., 2015). Interestingly, *in vitro* experiments have shown that the forces generated by kinesin-5 scale with microtubule overlap lengths, both pushing and braking force. This means that microtubules that slide faster relative to other filaments would experience a kinesin-5-dependent braking force, and slower filaments would experience a force that can accelerate their motion (Kapoor, 2017).

Eg5, one of the first known mitotic motor proteins, is a member of the kinesin-5 family (Le Guellec et al., 1991; Sawin et al., 1992). Kinesin-5 motors are crucial for generating forces for spindle pole separation and bipolar mitotic spindle formation (Zhu et al., 2005). However, to generate these forces Eg5 requires overlapping antiparallel microtubules (Ferenz et al., 2009). Besides overlapping microtubules, Eg5 localizes along spindle microtubules with enrichment near spindle poles and relocalizes to the midzone in late anaphase (Gable et al., 2010). However, since Eg5 concentration increases towards the poles that are comprised of lower density of antiparallel microtubules, its preference for antiparallel microtubules seems to be strange considering its physical localization within the spindle (Wojcik et al., 2013).

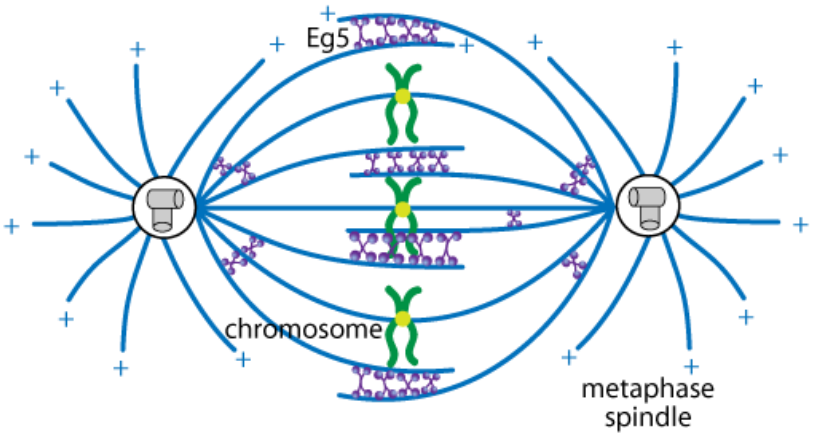

Figure 9. Schematic representation of the mitotic spindle and Eg5 cross-linking spindle microtubules (illustration adapted from Wojcik et al., 2013 by Cytoskeleton Inc., Denver, Colorado, US).

1.10. Dynein

The most abundant form of cytoplasmic dynein is a cytoplasmic dynein 1 (hereafter referred to as dynein) that drives the movement of a numerous discrete structures in all microtubule-containing cells towards the minus ends of microtubules (Allan, 2011). In mitosis, dynein localizes to multiple subcellular structures where it utilizes various functions – dynein is involved in chromosome movements, spindle organization, spindle positioning and checkpoint silencing. These activities imply poleward chromosome motility throughout mitosis by dynein's kinetochore transport toward the minus ends of spindle microtubules (Sharp et al., 2000), a kinetochore disassembly pathway that contributes to inactivation of the spindle checkpoint (Howell et al., 2001), centrosome separation during prophase (Tanenbaum et al., 2010), focusing the mitotic spindle poles via providing an essential stabilizing structure for the microtubule-centrosome interaction at the spindle pole (Radulescu and Cleveland, 2010), alignment of the mitotic spindle by tethering microtubules at the spindle poles (Merdes et al., 1996) and reorganization of prophase and prometaphase microtubule array (Rusan et al., 2002).

Recent *in vitro* studies revealed that dynein, beside crosslinking and bundling microtubules, can slide antiparallel ones (Tanenbaum et al., 2013). Interestingly, kinesin-5 (**Figure 10A**) and dynein (**Figure 10B**) have been shown to generate antagonistic forces on antiparallel microtubules in the spindle bipolarization, since dynein is thought to pull on antiparallel microtubules and favor spindle collapse (Mitchison et al., 2005; Tanenbaum et al., 2008; Ferenz et al., 2009). The combination of these two antagonistic forces is believed to be essential for bipolar spindle formation.

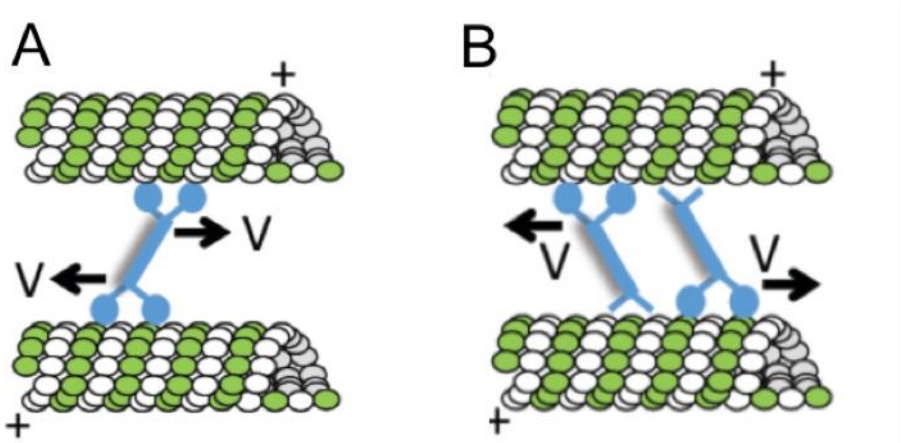

Figure 10. Representation of how dynein and kinesin-5 can crosslink and slide two microtubules apart. (A) A kinesin-5 homotetramer can walk towards the plus-end of each microtubule it crosslinks. (B) Dynein dimers can walk towards the minus-ends of the microtubules. Each motor domain in the dimer may interact with a different filament. Tubulin dimer is depicted as green-white subunits; motor proteins are blue; V stands for velocity; plus-ends of the microtubule are indicated (Kapoor, 2017).

1.11. Kinesin-4

One of the kinesins that shows enrichment at the spindle midzone is surely a member of the kinesin-4 family – Kif4A. This kinesin was the first kinesin observed to associate with mitotic chromosomes, thus termed chromokinesin (Wang and Adler, 1995). Analogous to other kinesins, Kif4A moves toward the plus ends of microtubules, but upon aggregation at the plus end, Kif4A reduces microtubule polymerization and depolymerization dynamics (Bringmann et al., 2004; Bieling et al., 2010).

At the onset of anaphase, Kif4A also localizes to the central part of now separating spindle and the midbody (Wang and Adler, 1995). Due to its localization, Kif4A is involved in various steps of the cell division, e.g. precise formation of the spindle midzone (Kurasawa et al., 2004; Zhu and Jiang, 2005).

Since PRC1 crosslinks antiparallel microtubules and was observed to decorate bridging fibers, it is of great importance to note that Kif4A is its binding partner. PRC1 works in tandem with Kif4A, known for translocation of PRC1 dimers to the plus-ends of microtubules, where consequently antiparallel microtubules are primarily crosslinked (Zhu et al., 2006).

Interestingly, depletion of Kif4A causes atypical elongation of the spindle midzone with unfocused overlap regions (Hu et al., 2011). Even though the localization of Kif4A at the spindle midzone is absent when PRC1 is depleted, PRC1 still localizes to the spindle midzone and the midbody when Kif4A is removed, although in a pattern that suggest longer overlap regions (**Figure 11**) (Zhu and Jiang, 2005). Presumably, this pattern of increased length of overlap regions occurs as PRC1 is not translocated to the plus-ends of microtubules, thereby having aberrant localization along microtubules. This observation is consistent with the *in vitro* observation that PRC1 and Kif4A have a combinatory effect in the regulation of the length of the anti-parallel overlap regions (Bieling et al., 2010).

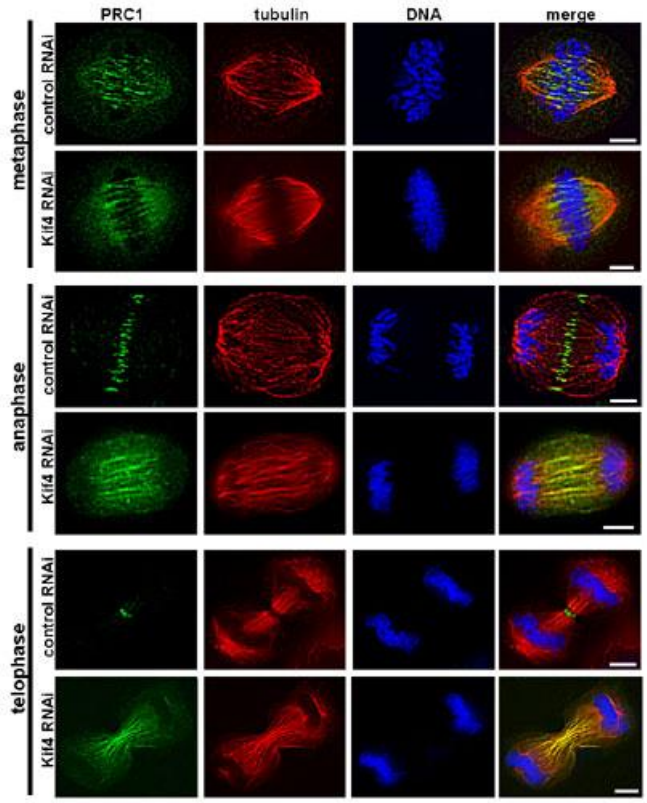

Figure 11. Differential pattern of localization of endogenous PRC1 in Kif4 esiRNA-treated cells. HeLa cells transfected with control esiRNA or Kif4 esiRNA were fixed and stained with rabbit anti-PRC1 antibodies (green), mouse anti-α-tubulin (red), and DAPI (DNA, blue). Scale bar, 5 μm (Zhu and Jiang, 2005).

1.12. Kinesin-6

The formation and function of the spindle midzone requires the activity of several members of the kinesin superfamily of motor proteins. Beside kinesin-4 that serves to translocate and organize a passive crosslinker PRC1, another family, namely kinesin-6, represents integral players in the formation and function of the spindle midzone. This family includes a microtubule plus-end directed motor protein, mitotic kinesin-like protein 1 (MKLP1), which via centralspindlin complex binds to PRC1 to reinforce the stability of the spindle midzone and enable anaphase (Lee et al., 2015).

In vitro experiments have shown that MKLP1 has plus end-directed microtubule motility to slide anti-parallel microtubules. Its localization within the mitotic spindle is at the spindle midzone, suggesting that MKLP1 slides the antiparallel microtubules of the two opposing poles apart (Nislow et al., 1990; Nislow et al., 1992). These proposed functions, cross-linking and sliding of antiparallel microtubules in the anaphase spindle, would generate forces to drive spindle elongation during anaphase B (Nislow et al., 1992).

Even though these experiments implicate the role of MKLP1 in the mitotic progression, recent studies indicated that MKLP1 functions specifically in cytokinesis, where as an integral factor controls the timing of midzone formation (Mishima et al., 2004). Immunofluorescence and live cell imaging revealed that depletion of MKLP1 does not affect the bundling of anti-parallel microtubules in the midzone (**Figure 12**). However, it prevents midbody formation and the completion of cytokinesis (Matuliene et al., 2002).

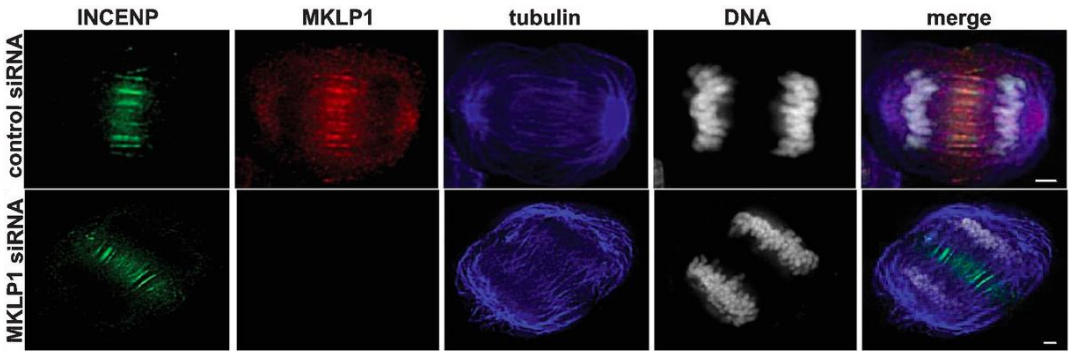

Figure 12. Suppression of MKLP1 expression by siRNA does not cause abnormality in midzone formation. HeLa cells grown on coverslips were transfected with control, or MKLP1 siRNA. Cells were fixed and stained with anti-inner centromere protein (INCEP) antibodies (green), anti-MKLP1 antibodies (red), anti-α-tubulin antibodies (blue) and DAPI to indicate DNA (white). Cells are shown in anaphase. Scale bars, 1 μm (Zhu et al., 2005).

1.13. Kinesin-13

Mitotic chromosome instability is eminently an aftermath of the disorder in the microtubule dynamics. Unlike other kinesins, the kinesin-13 family is a unique group of motor proteins that are non-motile, i.e. kinesin-13 family does not use the energy from ATP turnover to move directionally along microtubules. When binding to both the plus- and minus-ends of microtubules, members of kinesin-13 family promote destabilization of microtubules by depolymerizing tubulin subunits from the polymer end (Desai et al., 1999, Ogawa et al., 2004).

The kinesin-13 family has one of the integral roles in the regulation of microtubule dynamics (Wordeman, 2005; Howard and Hyman, 2007; Bakhoum et al., 2009; Tanenbaum et al., 2011). An extensively studied member of the family is the mitotic centromere-associated kinesin (MCAK), a kinesin-like protein Kif2C in humans encoded by the KI2C gene (Kim et al., 1998).

In context of the mitotic spindle, the localization of MCAK is in the cytoplasm throughout the cell cycle, specifically at the kinetochores, at the spindle poles and at the spindle midzone during mitosis (Wordeman and Mitchison, 1995; Maney et al., 1998; Walczak et al., 1996). Additionally, it was shown that MCAK displays differential localization to kinetochores throughout mitosis in which change of localization may be correlated with the kinetochore stretch and/or microtubule attachment (Kline-Smith et al., 2004).

Depletion of MCAK activity does not largely affect assembly of bipolar spindle (Zhu et al., 2005). However, depletion of MCAK activity results in perturbation of chromosome congression and segregation, perturbation of directionality of chromosome movement, severe segregation defects and improper kinetochore-microtubule attachment (Zhu et al., 2005; Kline-Smith et al., 2004). Notably, MCAK is required before anaphase onset to promote proper attachment of chromosomes to the mitotic spindle because if MCAK is depleted, defective attachments formed pre-anaphase are not solved and lead to segregation defects at anaphase (Kline-Smith et al., 2004). Thus, studies suggest that MCAK regulates microtubule dynamics to destabilize erroneous kinetochore-microtubule attachments.

1.14. Kinesin-8

Motor proteins play important roles in the formation of mitotic spindle, whether by controlling the stability of individual microtubules, or by cross-linking and sliding neighboring microtubules apart. Kinesin-8 family motors are major regulators controlling microtubule dynamics, which can utilize activities that lead to chromosome congression (Zhu et al., 2005). One of the kinesins-8 motors, Kif18A, translocates directionally along microtubules and depolymerizes stable microtubule plus-ends *in vitro* (Mayr et al., 2007). Unlike other kinesins, studies identified kinesin-8 as a dual-functioning kinesin, which has both motile and depolymerizing roles (Gupta et al., 2006).

Interestingly, length of a microtubule affects this depolymerization rate. Longer microtubules have faster depolymerization rate than shorter ones *in vitro* (Varga et al., 2006). Presumably, this length-dependent effect of kinesin-8 on the depolymerization rate is proportional to the amount of kinesin-8 motors moving toward the plus-ends, leading to greater accumulation on the plus-ends of longer microtubules than on shorter ones (Varga et al., 2006). This way, Kif18A would affect both spindle length and chromosome congression by regulating the plus-end dynamics of kinetochore microtubules (Mayr et al., 2007).

It was shown that Kif18A has an integral role in regulating oscillatory movements of the kinetochores by suppressing them. This leads to reduction in amplitude of pre-anaphase oscillations and slower poleward movement during anaphase (Stumpff et al., 2008). Thereby, suppressing chromosome movements. The extent of accumulation at plus-ends of k-fibers varies within the spindle, as it is more concentrated on k-fibers at the spindle periphery (Stumpff et al., 2008).

Interestingly, it was reported that budding yeast kinesin-8, Kip3, utilizes an anti-parallel microtubule-sliding activity that could potentially promote spindle assembly and increase the length of mitotic spindles (Su et al., 2013). Su et al. proposed “slide-disassemble” model where its sliding and destabilizing activity balance during pre-anaphase to facilitate a normal spindle assembly. These activities are also likely to be present in other eukaryotic cell types.

2. Materials and methods

2.1. Cell culture

HeLa-TDS cell line, permanently transfected and stabilized using pEGFP-α-tubulin plasmid was acquired from Mariola Chacón Rodríguez (Max Planck Institute of Molecular Cell Biology and Genetics, Dresden, Germany). HeLa-Kyoto BAC cell lines stably expressing protein PRC1-GFP, MKLP1-GFP, Eg5-GFP, DN1CH1-GFP, Kif18A-GFP or MCAK-GFP (Poser et al., 2008) were obtained from Hyman lab's BAC and Cell Line Database (Max Planck Institute of Molecular Cell Biology and Genetics, Dresden, Germany). Cells were cultured in filter sterilized Dulbecco's Modified Eagle's medium (DMEM; Lonza, Basel, Switzerland) with 10% Fetal Bovine Serum (FBS; Sigma-Aldrich, St. Louis, Missouri, US), 50 µg/mL geneticin (Santa Cruz Biotechnologies, Dallas, Texas, US) and 10000 U/mL penicillin-streptomycin (Lonza, Basel, Switzerland). Cells were grown at 37°C and 5% CO_2 in a Galaxy 170 R CO_2 humidified incubator (Eppendorf, Hamburg, Germany).

2.2. Transfection and RNA interference

For plasmid transfection and siRNA transfection, cells were transfected by electroporation using Amaxa Cell Line Nucleofector Kit R (Lonza, Basel, Switzerland) together with the Nucleofector 2b device (Lonza, Basel, Switzerland). Transfection was performed with A-028 (DSMZ) program by following the manufacturer's protocol. Cells were transfected with mCherry-PRC1 plasmid obtained from Casper C. Hoogenraad (University of Utrecht, Utrecht, The Netherlands) (van Beuningen et al., 2015). $1x10^6$ cells at 80% confluency were transfected with 1.5 µg of plasmid DNA. For PRC1 and Kif4A RNA interference, $1x10^6$ cells at 80% confluency were transfected with 100 nM targeting and control siRNA raw constructs diluted in 100 µL Nucleofector solution R (Lonza, Basel, Switzerland). The siRNA constructs were SMARTpool ON-TARGETplus PRC1 siRNA (#L-019491-00; Dharmacon, Lafayette, Colorado, US) and ON-TARGETplus Control Pool Non-targeting Pool (#D-001810-10-05; Dharmacon, Lafayette, Colorado, US), KIF4A

siRNA (h) (#sc-60888, Santa Cruz Biotechnologies, Dallas, Texas, US) and control siRNA-A (#sc-37007, Santa Cruz Biotechnologies, Dallas, Texas, US).

2.3. Immunostaining

For fixed cell imaging, cells were grown on 3.5-cm glass bottom microwell dishes (MatTek Corporation, Ashland, Massachusetts, US). Cells were fixed in -20°C methanol (100%) by putting the methanol directly on the cells and placing the cells on ice for 3 minutes. Methanol was washed off with 3 washes in 1x Phosphate Buffered Saline (PBS). Fixed cells were incubated in 0.5% Triton in 1x PBS for 15 minutes at room temperature while shaking gently on the shaker. Triton was washed off with 3 washes in 1x PBS, 5 minutes each wash. After permeabilization, cells were blocked in blocking buffer, 1% normal goat serum (NGS) in 1x PBS for one hour at 4°C while shaking gently on the shaker in the cold room. Blocking buffer was washed off with 3 washes in 1x PBS, 5 minutes each wash. Primary mouse monoclonal KIF4 (E-8) antibody (#sc-365144, Santa Cruz Biotechnologies, Dallas, Texas, US) of 200 µg/mL was prepared in blocking buffer as 1:100 dilution (Lee and Kim, 2005), 500 µL for each 3.5 cm dish. Primary antibody was added into the dish and the dish was put into a bigger Petri dish inlayed with a wet paper towel to prevent drying of antibody solution. Petri dish was sealed with parafilm. Cells were incubated with primary antibody for 24 hours in a cold room at 4°C. After 24 hours, the primary antibody was washed 3 times with 1x PBS, each wash 5 minutes at room temperature while shaking gently. Secondary goat anti-mouse antibody (AlexaFluor 647) (#ab150115, Abcam, Cambridge, UK) of 2 µg/µL was diluted in 2% NGS in 1x PBS to 1:1000 and added 500 µL of diluted secondary antibody on the cells. The dish was covered with aluminium foil and incubated for 1 hour at room temperature on the shaker. Secondary antibody was washed off with 3 washes in 1x PBS, 5 minutes each wash, while shaking gently. Imaging was done immediately after so 1x PBS was added to the sample to cover the cells and proceed with microscopy. Cells were protected from light until microscopy.

2.4. Sample preparation

To prepare samples for microscopy, following the transfection with plasmid or siRNA, DMEM medium was removed from the cells and the cells were rinsed with 1x PBS. 1 mL of 1% Trypsin/EDTA (Biochrom AG, Berlin, Germany) was added to the cells and the cells were incubated at 37°C and 5% CO_2 in a humidified incubator for 5 minutes. Trypsin was blocked when adding 5 mL of DMEM medium. Cells were counted using the Neubauer improved cell counting chamber (BRAND GMBH + CO KG, Wertheim, Germany). $2x10^5$ cells were seeded and cultured in 2 mL DMEM medium at 37°C and 5% CO_2 on 3.5-cm glass bottom microwell dishes. After 24 hours, the medium was replaced with Leibovitz's L-15 CO_2-independent medium (Lonza, Basel, Switzerland) supplemented with FBS. Live-cell imaging was done 3 hours after medium replacement. For experiments with the fixed samples, imaging was done immediately after immunostaining. 1 mL of 1x PBS was added to the sample to cover the cells and to proceed with microscopy. Cells were kept protected from light until microscopy. For live-cell staining of HeLa BAC cell lines SiR-tubulin dye (Cytoskeleton Inc., Denver, Colorado, US) was added to 2 mL of cells in a DMEM medium to a final concentration of 100 nM, 3 h before imaging.

2.5. Imaging

Cells were imaged using a Leica TCS SP8 X laser scanning confocal microscope (Leica, Wetzlar, Germany). The system was equipped with a HC PL APO 63x/1.4 oil immersion objective (Leica, Wetzlar, Germany) heated with an objective integrated heater system (Okolab, Pozzuoli, Italy). The system was controlled with the Leica Application Suite X software (LASX, 3.1.1.15751, Leica, Wetzlar, Germany) and Leica's TCS SP8 mode was used. During live cell imaging, cells were maintained at 37°C in Okolab stage top heating chamber (Okolab, Pozzuoli, Italy). To obtain the optimal balance between spatial resolution and signal-to-noise ratio, optical section was 0.896 and pinhole diameter was set to 1 AU. Excitation and emission lights were separated with Acousto-Optical Beam Splitter (Leica, Wetzlar, Germany). For cells expressing only GFP fused protein and stained with SiR-tubulin, a 488 nm Argon

laser line was used for GFP excitation and a 649 nm white light laser (WLL) for SiR-tubulin. GFP emissions were detected with the first hybrid detector (HyD) in the range of 493-639 nm, whilst SiR-tubulin emissions were detected with the second HyD detector in the range of 654-779 nm. For cell expressing both GFP and mCherry fused proteins, a 488 nm Argon laser line was used for GFP excitation and a 587 nm WLL for mCherry excitation. In these cells, GFP emissions were detected with the first HyD detector in the range of 493-582 nm, whilst mCherry emissions were detected with the second HyD detector in the range of 592-780 nm. Ultimately, for cells expressing GFP, immunostained with AlexaFluor647-antibody, a 488 nm Argon laser line was used for GFP excitation and a 653 nm WLL for AlexaFluor647. GFP emissions were detected with the first HyD detector in the range of 493-639 nm, whilst AlexaFluor647 emissions were detected with the second HyD detector in the range of 658-779 nm. In time-lapse imaging, films were acquired at one focal plane during 10-20 minutes with time interval set to 1 minute and 400 Hz unidirectional xyt scan mode. For fixed cell imaging, z-stacks were acquired comprising 3-6 focal planes with 0.5 µm-spacing and 400 Hz unidirectional xyz scan mode. All images were obtained with line averaging set to 16 and pixel size set to 50 nm.

2.6. Image analysis

After microscopy, image analysis and processing were performed in ImageJ (National Institutes of Health, Bethesda, Maryland, US). Quantification, graphing, data and statistical analysis were performed in RStudio (RStudio Inc., Boston, Massachusetts, US). Statistical analysis was performed using Student's t-test. Data are given as mean ± standard error of the mean (s.e.m.). Images in figures were rotated so the spindle long axis in images is aligned horizontally, and ImageJ was used to adjust brightness and contrast. Images and legend for figures were assembled in Adobe Illustrator CC (Adobe Systems, Mountain View, California, US).

In HeLa cells stained with SiR-tubulin, 5-pixel-thick pole-to-pole contour of tubulin signal was tracked along the sister k-fibers and the corresponding bridging fiber that bridges the gap between sister k-fibers (**Figure 13**). The positions of the spindle poles were estimated as the merging points of k-fibers. To track the bundles, segmented line tool was used, point-by-point along the curved line of tubulin signal. When tracks were placed, intensity profiles were acquired in the green channel for Eg5-GFP, DN1CH1-GFP, MCAK-GFP, MKLP1-GFP and Kif18A-GFP.

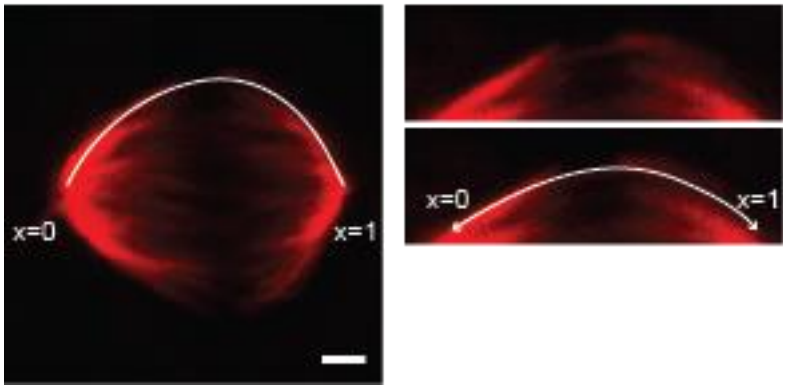

Figure 13. Pole-to-pole tracking. Images show pole-to-pole tracking of SiR-tubulin signal by following the curve of sister k-fiber in the red channel. Enlargements show the region of interest where corresponding bridging fiber spans the gap between sister k-fibers. Intensity profiles were acquired in green, GFP channel. x=0 represents first, while x=1 represents second spindle pole, respectively.

In cells stably expressing PRC1-GFP, PRC1-labeled bundle contour was tracked from pole-to-pole. PRC1-GFP intensity profile was acquired in green channel, while Kif4A-Alexa Fluor-647 intensity profile was acquire in red channel, respectively. In cells transfected with mCherry-PRC1, mCherry-PRC1 intensity profile was acquired in red channel, while MKLP1-GFP intensity profile was acquired in green channel. The mean value of the cytoplasm background was subtracted from the intensity profiles. The length of tracked overlap bundles was calculated as the width of the peak in the intensity profile, positioned in the central part of the contour (**Figure 14**).

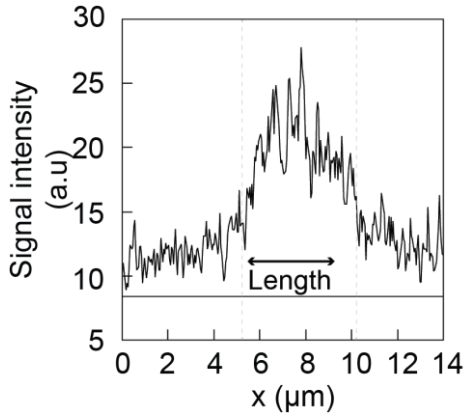

Figure 14. Example of length measurement of the MKLP1-GFP signal. Intensity profile acquired with pole-to-pole tracking of SiR-tubulin signal in a HeLa cell stably expressing MKLP1-GFP. Length was calculated as the width of the peak at its base. Left vertical dashed line shows the lower limit of calculation, whereas right shows the upper limit, respectively. Horizontal line shows mean background of the cytoplasm.

The signal intensity of a cross section of a bridging fiber was measured by drawing a 5-pixel line, perpendicular to the spindle long axis, at the central part of the bridging fiber. The mean value of the cytoplasm background was subtracted from the intensity profiles and the signal intensity was calculated as the area under the peak (**Figure 15**). Similarly, Kif18A-GFP punctae intensities were measured as the area under Kif18A-GFP peaks from pole-to-pole intensity profile.

Spindle length was measured as the distance between the spindle poles, whereas spindle width was measured as the distance between midpoints of outermost PRC1-labeled fibers on the opposite spindle poles.

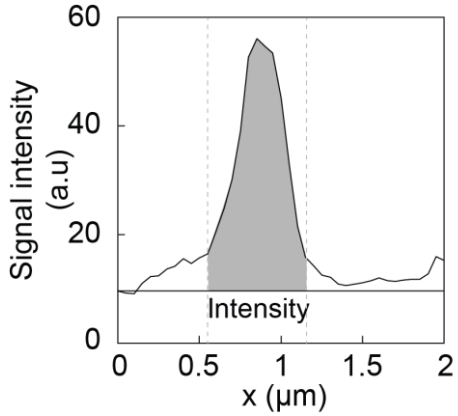

Figure 15. Example of a cross section signal intensity of PRC1-GFP bundle. Intensity profile acquired at the central part of PRC1-GFP-labeled bundle with line perpendicular to the spindle long axis in a HeLa cell stably expressing PRC1-GFP. Left vertical dashed line shows lower limit of calculation, while right shows upper limit, respectively. Horizontal line shows mean background of the cytoplasm subtracted from the intensity profile. Intensity was calculated as the area under the peak

3. Results

3.1. Eg5 localizes to the spindle poles and k-fibers

To identify the localization of human kinesin-5 with respect to the bridging fibers, HeLa cells stably expressing Eg5-GFP from a bacterial artificial chromosome (BAC) were stained with SiR-tubulin dye. Time series that cover transitions through phases of mitosis were acquired. Acquired images show that only a small portion of the molecules is diffused in the cytoplasm. From prometaphase to late anaphase, Eg5-GFP is predominantly localized in the mitotic spindle (**Figure 16**). The localization of Eg5-GFP follows the localization of SiR-tubulin, with no apparent reduction or increase in the overall signal intensity through phases. Intensity profiles show that Eg5-GFP is highest at the spindle poles and gradually decreases toward the plus ends of the k-fibers, i.e. toward the kinetochores. At the central part of the spindle where antiparallel microtubules interdigitate from opposing poles, Eg5-GFP signal is the lowest (**Figure 17**). Upon investigation of metaphase spindles, no Eg5 signal was observed to extend to the region between k-fibers where bridging fiber resides. However, as cell progresses through mitosis, Eg5 slightly accumulates at the lateral parts of the spindle midzone.

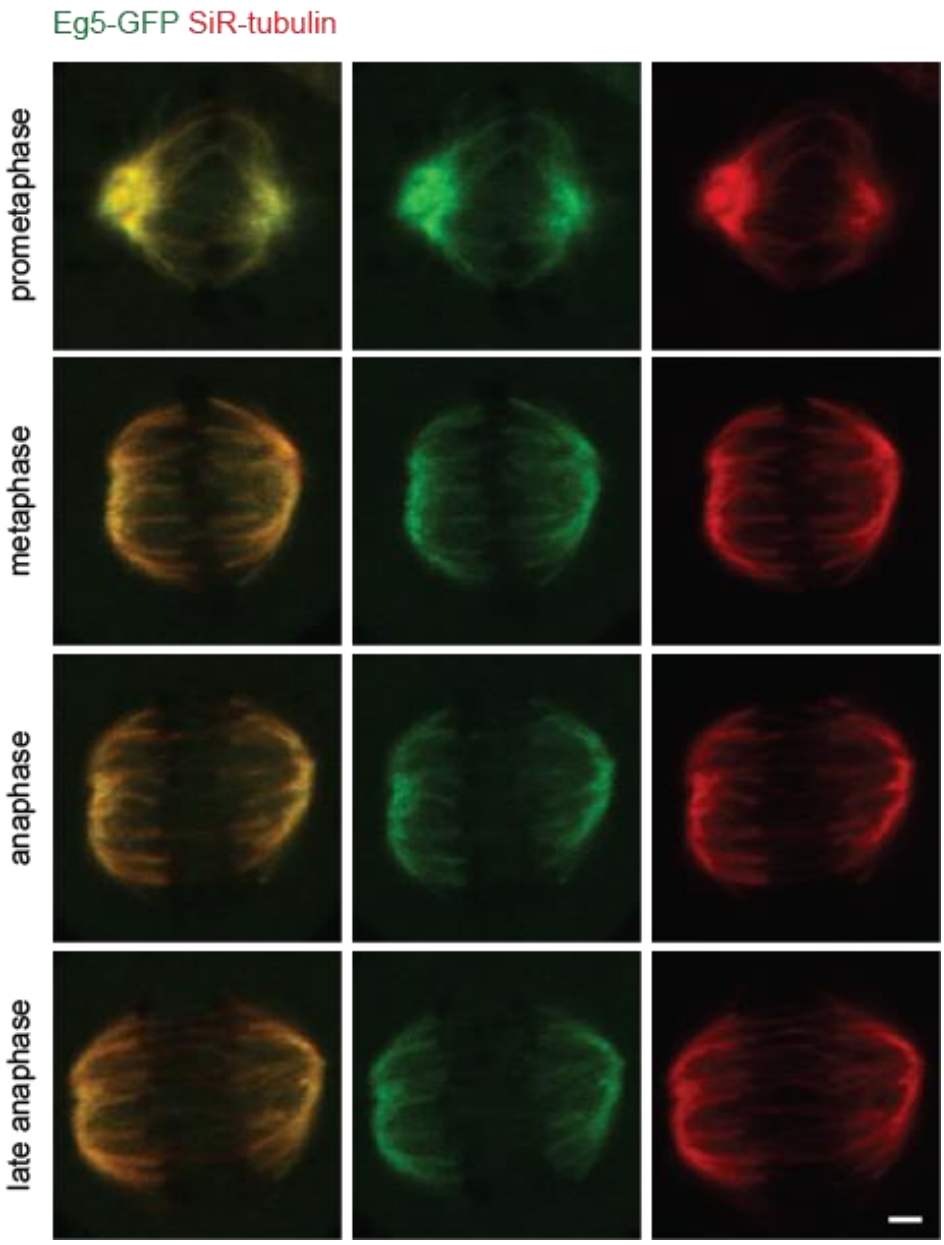

Figure 16. Localization of Eg5-GFP in the prometaphase, metaphase, anaphase and late anaphase spindle. HeLa cells stably expressing Eg5-GFP (green) and stained with SiR-tubulin dye (red). One z-slice for each spindle is shown. Images (left: merge, middle: GFP, right: SiR-tubulin) of spindles are as follows: first row shows spindle in prometaphase, second metaphase, third anaphase and fourth late anaphase. Scale bar, 2 μm.

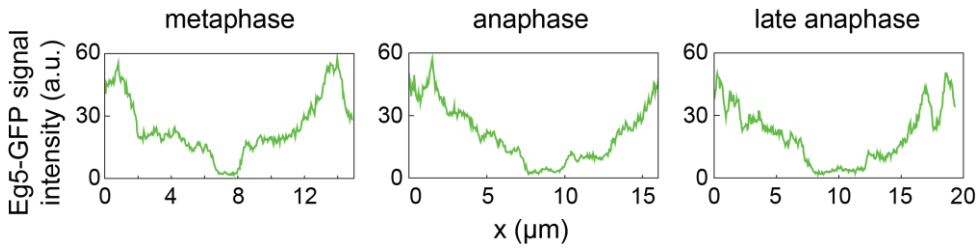

Figure 17. Eg5-GFP intensity profiles. Graphs show pole-to-pole intensities (green) of Eg5-GFP signal acquired in HeLa cells expressing Eg5-GFP and stained with SiR-tubulin. Intensity profiles are tracked in metaphase (left), anaphase (middle), and late anaphase (right) spindle.

3.2. Localization of MKLP1 in the central part of the spindle

HeLa cells stably expressing MKLP1-GFP, a kinesin-6 motor, were stained with SiR-tubulin. As seen in Figure 18, MKLP1-GFP is localized in the spindle throughout mitosis. However, large portion of the molecules is diffused through the cytoplasm. The localization of MKLP1-GFP at the spindle increases as the cell progresses through mitosis, having the highest signal at the latter stages. In prometaphase, MKLP1-GFP is accumulated at the plus ends of microtubules, being highest in the bundled microtubules. Interestingly, pole-to-pole intensity profiles of MKLP1-GFP localization showed enrichment in the central part of the spindle as the metaphase began (**Figure 18**). Progressing from metaphase to late anaphase, intensity profiles show the increase in the width of the peak at the spindle midzone and the overall signal intensity (**Figure 19**). The length of the metaphase MKLP1-GFP signal calculated from pole-to-pole intensity profile was 4.09 ± 0.15 µm (n=18 tracks from 9 cells), less than the length of the overlap regions of bridging fibers reported by Kajtez et al., 2016. However, MKLP1-GFP signal was observed to extend to both the gap region between sister k-fibers and laterally from estimated positions of the kinetochores in metaphase spindles (**Figure 18**).

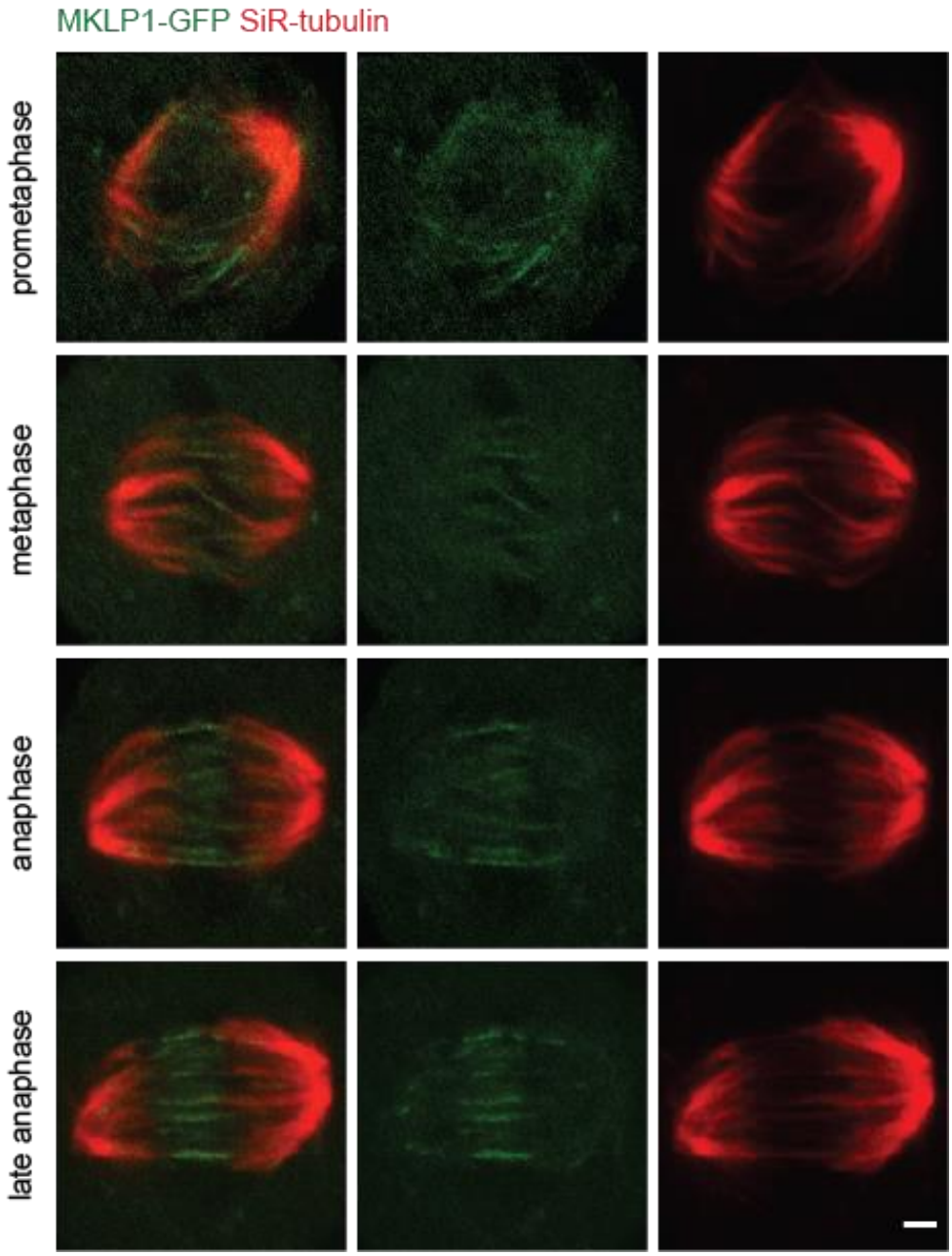

Figure 18. Localization of MKLP1-GFP in the prometaphase, metaphase, anaphase and late anaphase spindle. HeLa cells stably expressing MKLP1-GFP (green) and stained with SiR-tubulin dye (red). One z-slice for each spindle is shown. Images (left: merge, middle: GFP, right: SiR-tubulin) of spindles are as follows: first row shows spindle in prometaphase, second metaphase, third anaphase and fourth late anaphase. Scale bar, 2 µm.

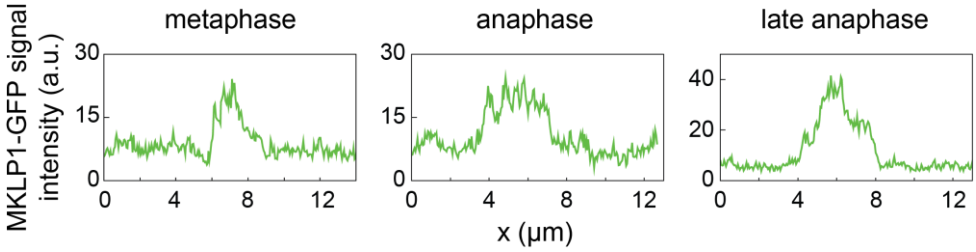

Figure 19. MKLP1-GFP intensity profiles. Graphs show pole-to-pole intensities (green) of MKLP1-GFP signal acquired in HeLa cells expressing MKLP1-GFP and stained with SiR-tubulin. Intensity profiles are tracked in metaphase (left), anaphase (middle), and late anaphase (right) spindle.

3.3. Kif18A is localized at the plus ends of microtubules of the k-fibers

To determine localization of human kinesin-8 through the phases of mitosis, HeLa cells stably expressing Kif18A-GFP were stained with SiR-tubulin dye. In prometaphase, Kif18A-GFP is observed as a diffuse signal all over the spindle. At the onset of metaphase, diffused signal from prometaphase spindles accumulates at the plus ends of microtubules, whilst forming Kif18A-GFP punctae at the plus ends of the k-fibers, i.e. where kinetochores are positioned (**Figure 20**). These Kif18A-GFP punctae diminished as cell proceeded to anaphase. Intensity profiles show that as Kif18A-GFP punctae signal decreased, new peak emerged in the central part of now separating spindle (**Figure 21**). Therefore, Kif18A-GFP is translocated to the antiparallel regions as poles separate. Contrary, pole-to-pole tracking revealed no peak at the central part of the metaphase spindle, between Kif18A-GFP punctae. Thus, no Kif18A signal is present in the region between estimated kinetochore positions in the metaphase spindle. Interestingly, pole-to-pole intensity profiles of Kif18A-GFP in metaphase spindle show distinction between outer and inner sister k-fibers (**Figure 22**). K-fibers located more than 3 µm away from the spindle long axis have both Kif18A-GFP punctae present, while 70% of inner ones has only one Kif18A-GFP punctus (n=47 in 10 cells).

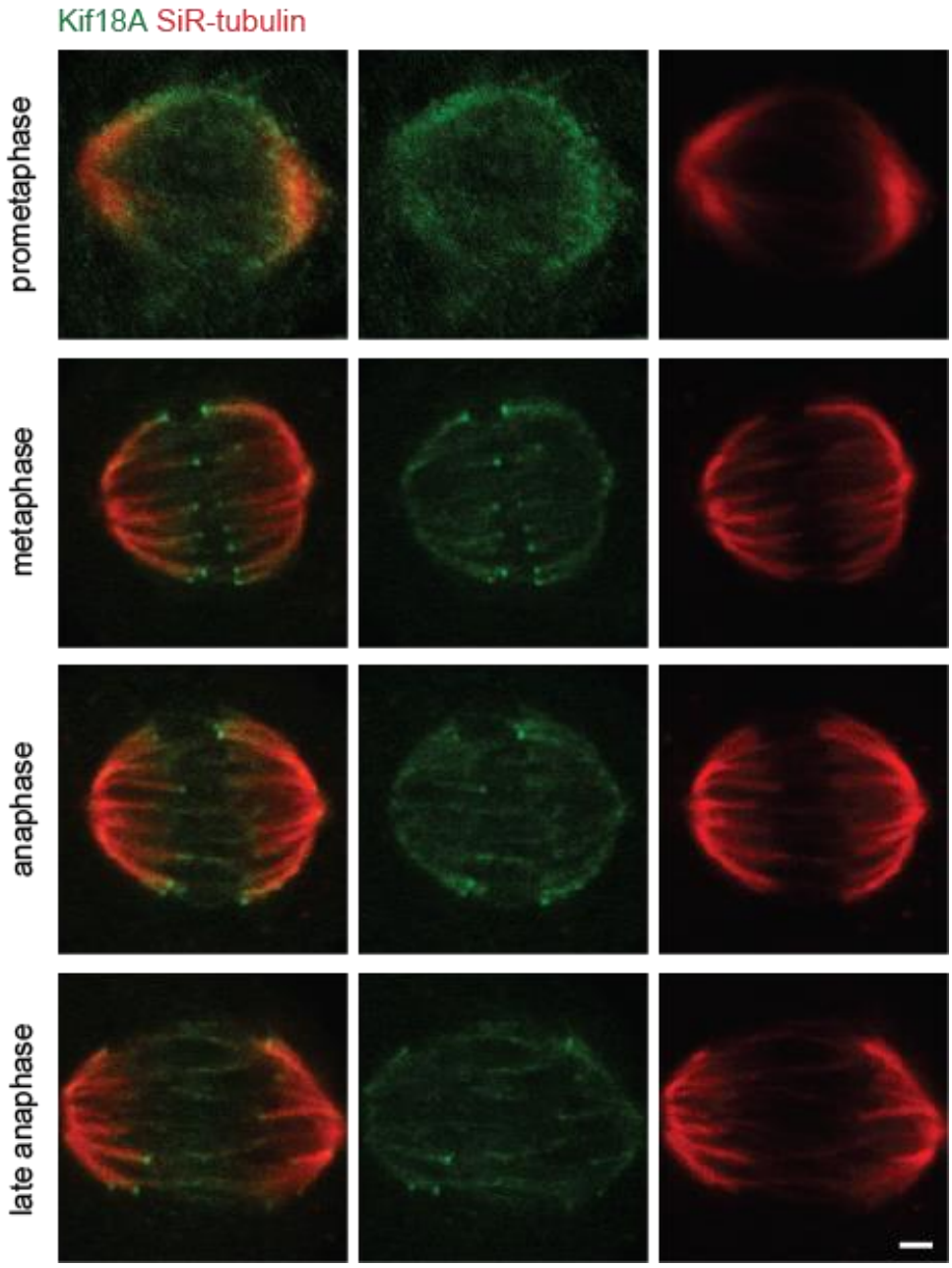

Figure 20. Localization of Kif18A-GFP in the prometaphase, metaphase, anaphase and late anaphase spindle. HeLa cells stably expressing Kif18A-GFP (green) and stained with SiR-tubulin dye (red). One z-slice for each spindle is shown. Images (left: merge, middle: GFP, right: SiR-tubulin) of spindles are as follows: first row shows spindle in prometaphase, second metaphase, third anaphase and fourth late anaphase. Scale bar, 2 μm.

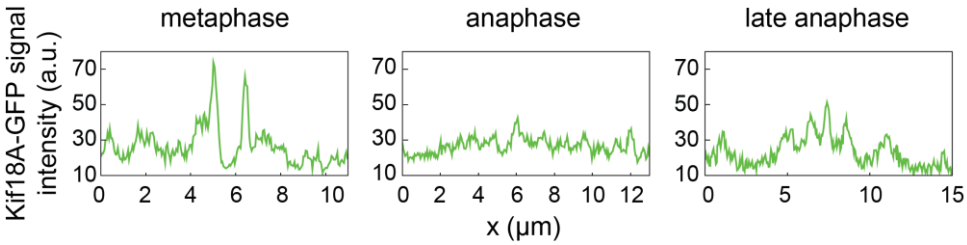

Figure 21. Kif18A-GFP intensity profiles. Graphs show pole-to-pole intensities (green) of Kif18A-GFP signal acquired in HeLa cells expressing Kif18A-GFP and stained with SiR-tubulin. Intensity profiles are tracked in metaphase (left), anaphase (middle), and late anaphase (right) spindle.

Additionally, intensity of the outer Kif18A-GFP punctae is statistically larger than that of inner ones (**Figure 22C**). Intensity of the outer Kif18-GFP punctae was 25.502 ± 2.16 a.u. (n=22 punctae in 10 cells), whereas intensity of inner punctae was 18.42 ± 2.213 a.u. (n=25 punctae in 10 cells).

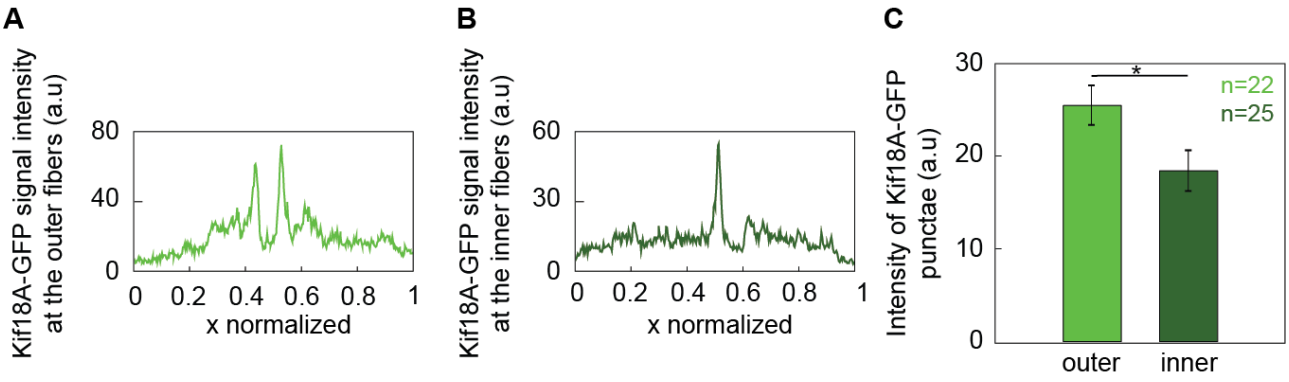

Figure 22. Kif18A-GFP intensity profiles at the outer and inner fibers. (A-B) Graphs show pole-to-pole intensities of Kif18A-GFP signal acquired in HeLa cells expressing Kif18A-GFP and stained with SiR-tubulin. (A) Normalized pole-to-pole intensity profiles acquired at outer (light green) sister k-fibers and (B) inner (dark green) sister k-fibers, respectively. (C) Intensity of the outer Kif18A-GFP punctae (light green) and inner (dark green). Intensities were measured in 10 cells, 22 punctae at the distance larger than 3 μm from the spindle log axis and 25 punctae positioned in less than 3 μm from the spindle long axis. P-value, 0.0279.

3.4. MCAK-GFP localizes to both spindle poles and kinetochores

HeLa cells stably expressing MCAK-GFP, a human kinesin-13 protein, were stained with SiR-tubulin. Unlike other kinesins, MCAK-GFP is observed at both kinetochores, suggesting positions of the plus ends of the microtubules, and at the poles, suggesting position of the minus ends of the microtubules (**Figure 23**). Beside its localization to the spindle throughout mitosis, large portion of MCAK-GFP molecules is diffused in the cytoplasm. In the spindle, MCAK-GFP showed no reduction or increase in the overall signal intensity. In prometaphase, MCAK-GFP has highest signal at the both poles and unaligned kinetochores. Same localization is observed in metaphase when kinetochores are aligned, together with low intensity all over k-fibers (**Figure 24**). Upon investigation, regions between sister k-fibers and estimated sister kinetochores showed no enrichment in MCAK in metaphase spindle. However, when poles start to separate, MCAK-GFP starts to accumulate to the central part of the spindle, i.e. to the spindle midzone.

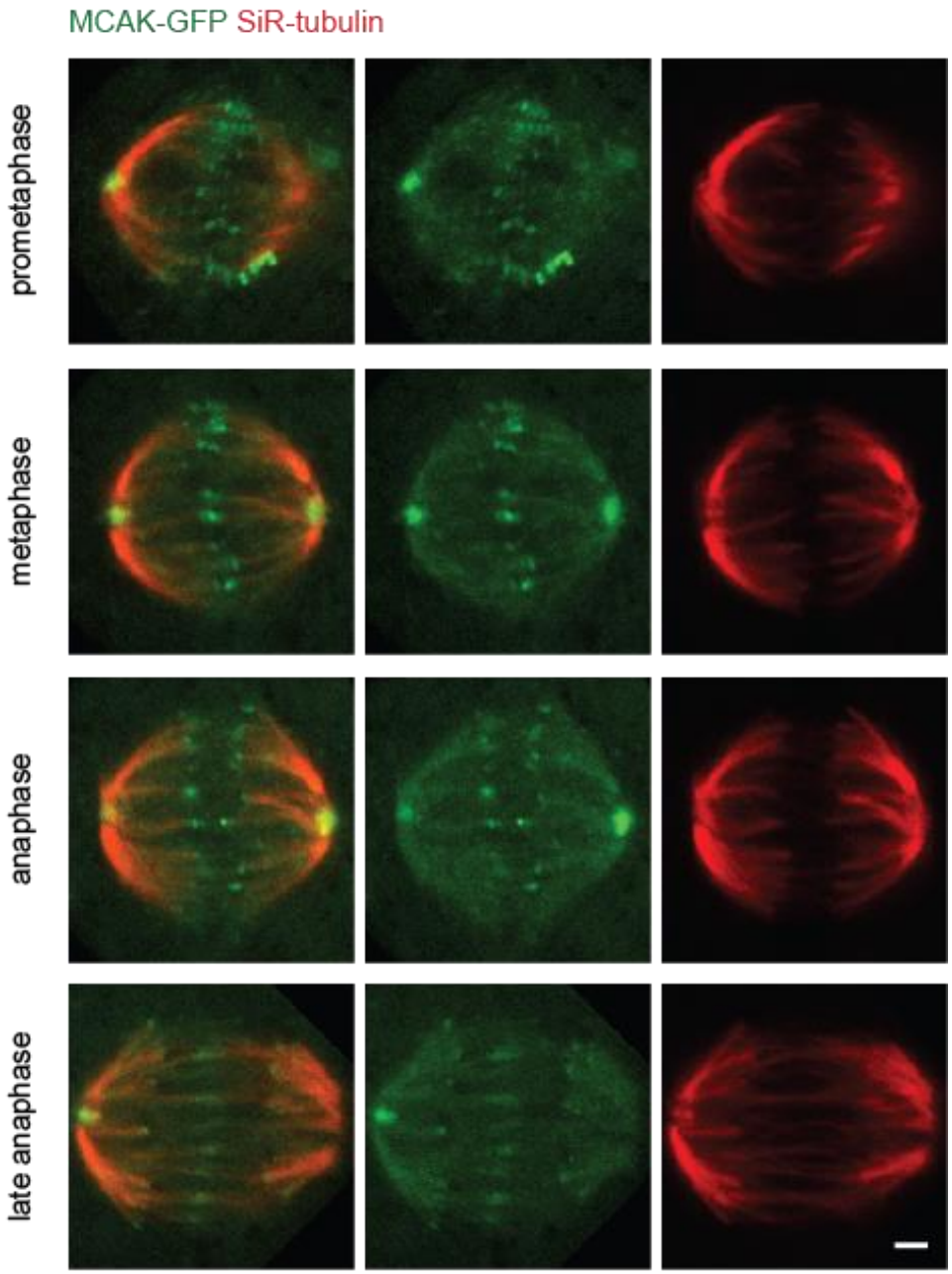

Figure 23. Localization of MCAK-GFP in the prometaphase, metaphase, anaphase and late anaphase spindle. HeLa cells stably expressing MCAK-GFP (green) and stained with SiR-tubulin dye (red). One z-slice for each spindle is shown. Images (left: merge, middle: GFP, right: SiR-tubulin) of spindles are as follows: first row shows spindle in prometaphase, second metaphase, third anaphase and fourth late anaphase. Scale bar, 2 µm.

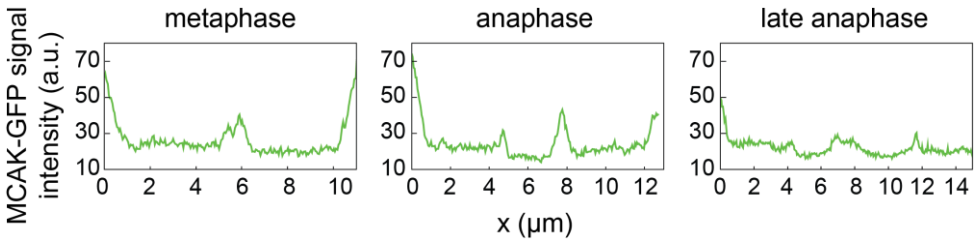

Figure 24. MCAK-GFP intensity profiles. Graphs show pole-to-pole intensities (green) of MCAK-GFP signal acquired in HeLa cells expressing MCAK-GFP and stained with SiR-tubulin. Intensity profiles are tracked in metaphase (left), anaphase (middle), and late anaphase (right) spindle.

3.5. Kif4A is localized at the chromosome and accumulates at the spindle midzone in anaphase

HeLa cells stably expressing PRC1-GFP, protein observed within bridging fibers, were fixed and immunostained for kinesin-4, Kif4-A. Kif4A, as chromokinesin, is predominantly observed at the chromosomes throughout the mitosis (**Figure 25**). In prometaphase, I observed that Kif4A also localizes in the PRC1-labeled bundles. Due to highest signal of Kif4A-Alexa Fluor-647 at the chromosomes, which are in metaphase aligned in the central part of the spindle, localization at the bridging fiber cannot be observed. However, as chromosomes separate and move toward the poles, Kif4A can be seen in the central part of the spindle, at the positions of PRC1-labeled antiparallel regions. Proceeding to cell division, Kif4A signal intensity in these narrow streaks increases (**Figure 26**).

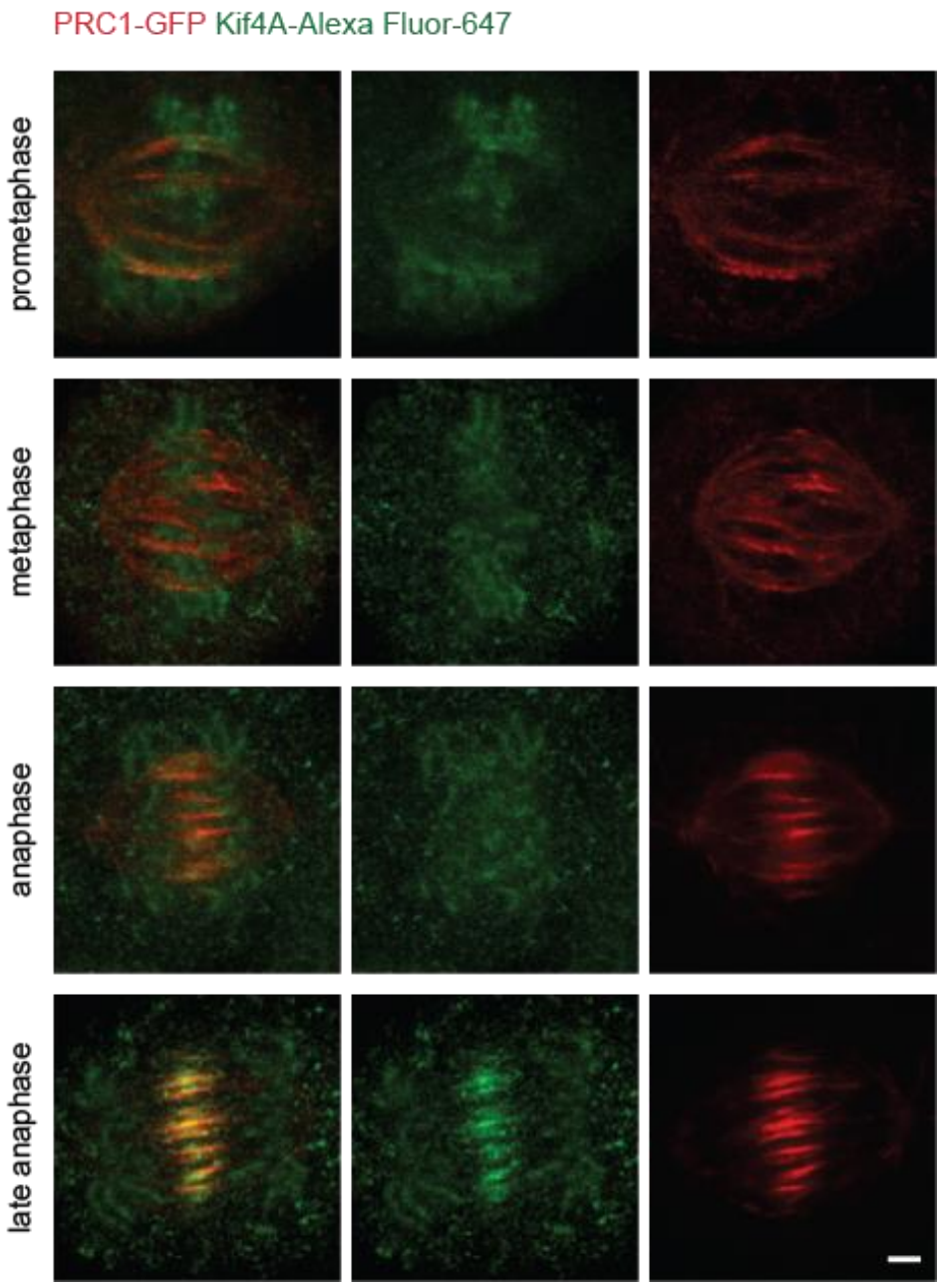

Figure 25. Localization of endogenous Kif4A in the prometaphase, metaphase, anaphase and late anaphase spindle. HeLa cells stably expressing PRC1-GFP (red) and immunostained for Kif4A (green). One z-slice for each spindle is shown. Images (left: merge, middle: Alexa Fluor-647, right: GFP) of spindles are as follows: first row shows spindle in prometaphase, second metaphase, third anaphase and fourth late anaphase. Scale bar, 2 μm.

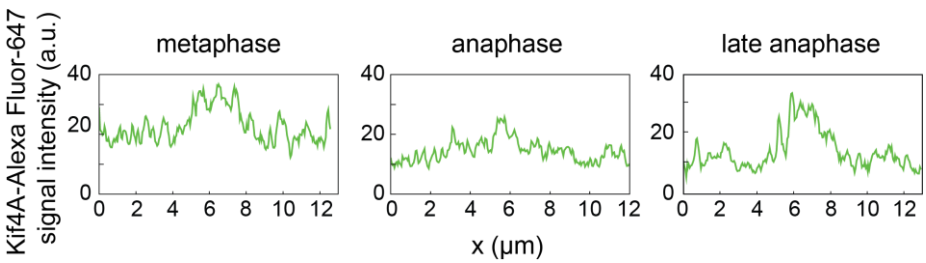

Figure 26. Kif4A-Alexa Fluor-647 intensity profiles. Graphs show pole-to-pole intensities (green) of endogenous Kif4A signal acquired in fixed HeLa cells expressing PRC1-GFP and immunostained for Kif4A (Alexa Fluor-647). Intensity profiles are tracked in metaphase (left), anaphase (middle), and late anaphase (right) spindle.

3.6. Dynein

To characterize the localization of the minus end motor protein, dynein, HeLa cells stably expressing DN1CH1-GFP were used. Tubulin was stained with SiR-tubulin to visualize microtubules and thus enable identification within the spindle. DN1CH1-GFP signal was observed throughout cytoplasm and at the cell cortex. In prometaphase, DN1CH1-GFP is localized at the estimated positions of kinetochores, causing poleward chromosome motility, and at the spindle poles where it stabilizes microtubule-centrosome interaction (**Figure 27**). Contrary to kinesins, DN1CH1-GFP had weak association with the spindle, and was primarily localized at the spindle poles in metaphase, where minus ends of the microtubules reside. Low signal intensities of DN1CH1-GFP were also observed at the k-fibers. To determine whether DN1CH1-GFP is localized in the bridging fibers of the metaphase spindle, SiR-tubulin signal that spans the region between sister k-fibers was followed. Upon inspection, no localization of DN1CH1 was observed at the positions of the bridging fibers (**Figure 28**).

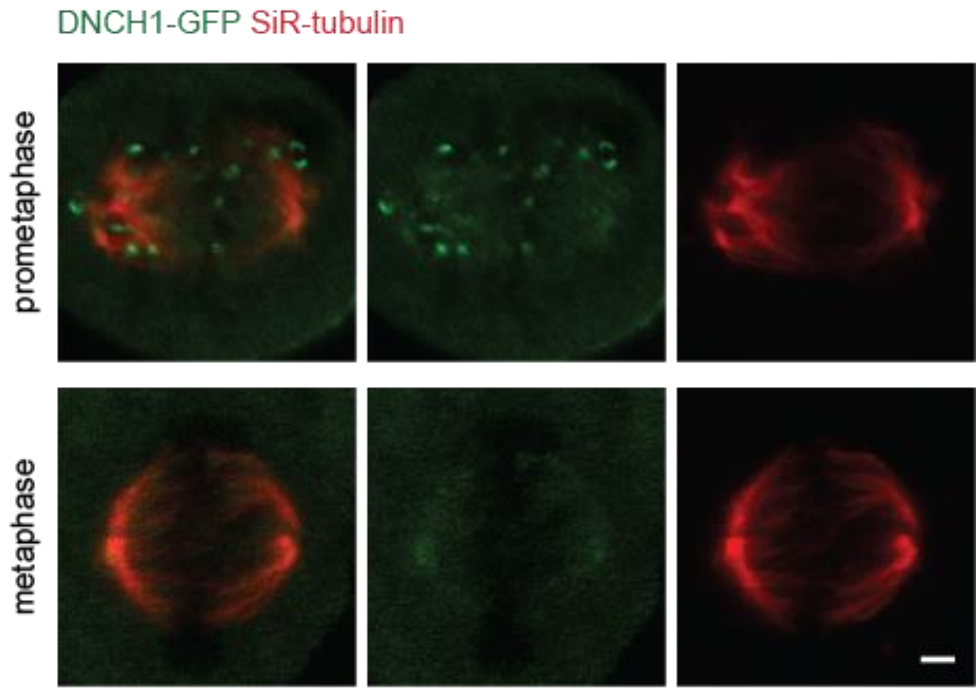

Figure 27. Localization of DN1CH1-GFP in the prometaphase and metaphase spindle. HeLa cells stably expressing DN1CH1-GFP (green) and stained with SiR-tubulin dye (red). One z-slice for each spindle is shown. Images (left: merge, middle: GFP, right: SiR-tubulin) of spindles are as follows: first row shows spindle in prometaphase, and second in metaphase. Scale bar, 2 µm.

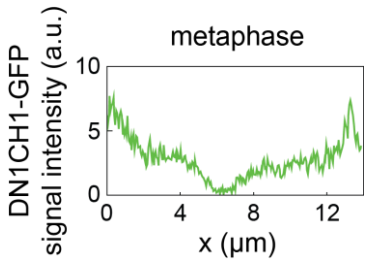

Figure 28. DN1CH1-GFP intensity profile. Graph shows pole-to-pole intensity (green) of DN1CH1-GFP signal acquired in HeLa cell expressing DN1CH1-GFP and stained with SiR-tubulin. Intensity profile is tracked in metaphase.

3.7. PRC1 overexpression causes aberrant relocalization of motor proteins

PRC1 can be used to visualize the overlap regions of bridging microtubules throughout the spindle. However, how does overexpression of PRC1 affect the localization of motor proteins is unknown. HeLa cells stably expressing DN1CH1-GFP, Kif18A-GFP, MKLP1-GFP, Eg5-GFP, MCAK-GFP and tubulin-GFP (for Kif4A experiment) were transfected with mCherry-PRC1 plasmid. Upon investigation, it was observed that mCherry-PRC1 overexpression results in aberrant relocalization of namely all inspected motor proteins. With PRC1 being overexpressed, motor proteins seem to associate with overlap bundles (**Figure 29, 30**).

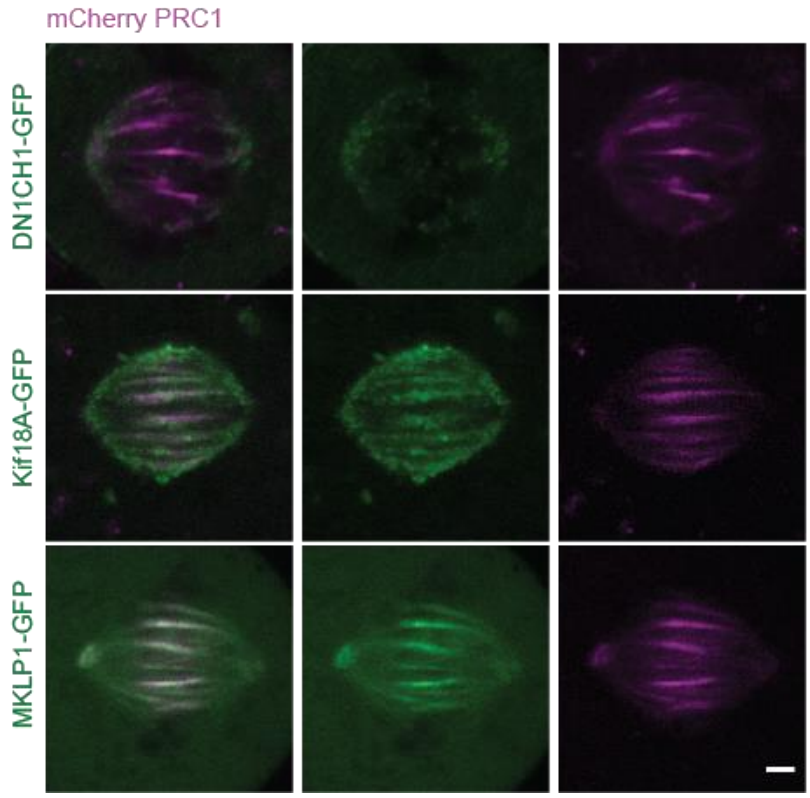

Figure 29. Overexpression of PRC1 in DN1CH1-GFP, Kif18A-GFP, and MKLP1-GFP cell lines. HeLa cells stably expressing DN1CH1-GFP (first row), Kif18A-GFP (second row) and MKLP1-GFP (third row) transfected with mCherry-PRC1 plasmid. One z-slice for each spindle is shown. Images are left: merge, middle: GFP, and right: mCherry, respectively. Scale bar, 2 μm.

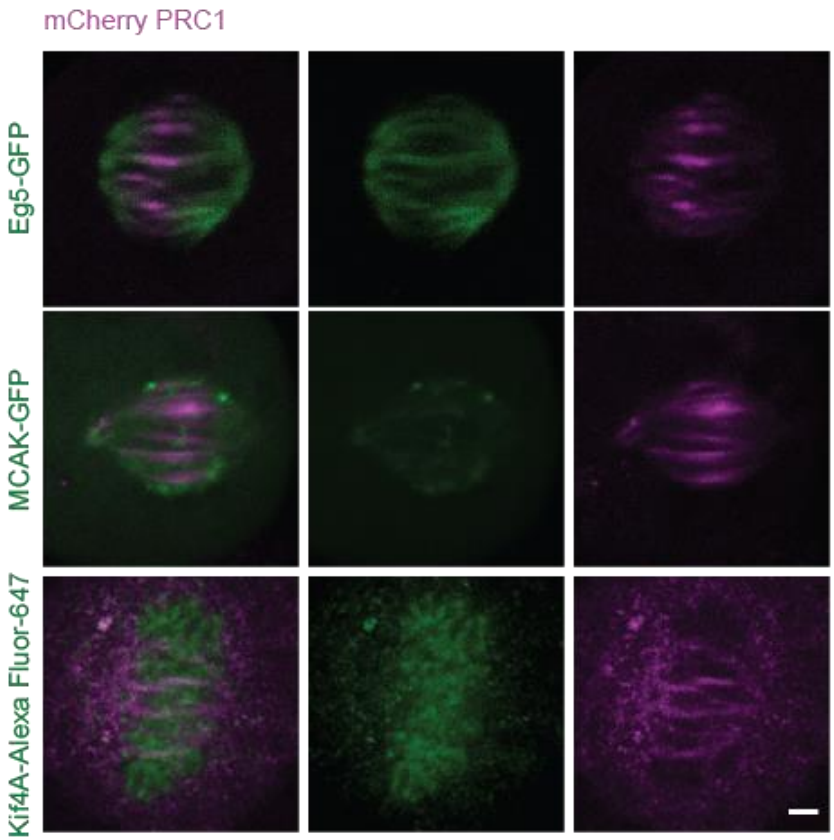

Figure 30. Overexpression of PRC1 in Eg5-GFP, MCAK-GFP, and tubulin-GFP cell lines. HeLa cells stably expressing DN1CH1-GFP (first row), Kif18A-GFP (second row) and tubulin-GFP (third row) transfected with mCherry-PRC1 plasmid. Tubulin-GFP transfected with mCherry-PRC1 plasmid was immunostained for Kif4A (tubulin not shown). One z-slice for each spindle is shown. Images for upper two row are left: merge, middle: GFP, and right: mCherry, respectively. Images for bottom row are left: merge, middle: Alexa Fluor-647, and right: mCherry. Scale bar, 2 µm.

This atypical change of localization is presumably the consequence of substantial crosslinking of all neighboring microtubules in the PRC1-labeled overlap bundles. Unlike kinesins, minus-end motor DN1CH1 did not undergo this change of localization. Beside relocalization of kinesins to the overlap bundles, cells were unable to properly align chromosomes and were therefore blocked in prometaphase.

3.8. MKLP1-labeled bundles correlate with PRC1-labeled bundles

As shown above, the localization of MKLP1 was observed in the central part of the spindle, similar to the localization of PRC1-labeled bridging fibers, as reported in Polak et al., 2017. However, localization of MKLP1 in the central part of the spindle does not reveal presence in the bridging fibers. To explore if MKLP1 is indeed localized within bridging fibers, overexpression of PRC1 should affect distribution of MKLP1 in the bridging fiber as it would affect bridging fibers themselves. HeLa cells stably expressing MKLP1-GFP and transfected with mCherry-PRC1 that showed normal alignment of chromosome at the metaphase plane were taken for determination of this relationship.

Pole-to-pole intensity profiles of MKLP1-labeled bundles and PRC1-labeled bundles were used to measure the length and the thickness of the corresponding signal. I found that both parameters of MKLP1-labeled bundles correlate with both parameters of PRC1-labeled bundles (**Figure 31**). Additionally, their length and thickness of the bundles were observed to be statistically similar. Length of the MKLP1-GFP signal was 4.768 ± 0.183 μm and mCherry-PRC1 was 4.780 ± 0.187 μm ($p=0.963$, $n=20$ bundles in 7 cells), whereas thickness of the MKLP1-labeled bundle was 0.617 ± 0.02 μm and mCherry-PRC1 was 0.618 ± 0.02 μm ($p=0.0996$, $n=15$ bundles in 7 cells). Since these parameters correlate with PRC1 overexpression, MKLP1 is localized within the bridging fiber.

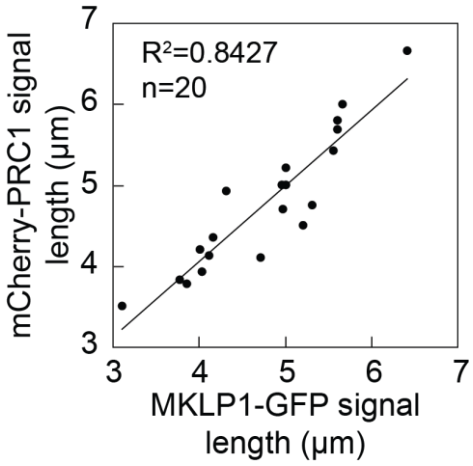

Figure 31. Correlation between MKLP1- and PRC1-labeled bundles. Graph shows correlation between length of the MKLP1-GFP signal and mCherry-PRC1 signal length in HeLa cells stably expressing MKLP1-GFP and transfected with mCherry-PRC1 plasmid. P-value, 0.00001.

3.9. Kif4A knockdown results in elongated bridging fibers.

Previous studies reported that silencing of Kif4A results in the spindle midzone with unfocused overlap regions and atypical elongation of the spindle midzone (Hu et al., 2011). Since PRC1 still localizes to the spindle midzone and the midbody when Kif4A is removed I set out to determine how it affects the bridging fibers. HeLa cells stably expressing PRC1-GFP were transfected with control siRNA and siRNA targeting Kif4A (**Figure 32**). To confirm silencing of Kif4A, cells were also fixed and immunostained for Kif4A.

To inspect the changes of the overlap regions in the bridging fibers induced by Kif4A knockdown, pole-to-pole PRC1-GFP signal intensities were acquired. Upon measurement, length of PRC1-labeled bundles was increased in cells treated with Kif4A siRNA when comparing to control cells (**Figure 33**). In control cells, the length of PRC1-GFP signal was 4.714 ± 0.189 µm (n=20 in 9 cells). However, in cells treated with Kif4A siRNA, the length of PRC1-GFP signal was 5.527 ± 0.279 µm (p=0.021, n=20 in 8 cells). These data confirm the elongation of PRC1-labeled bundles and therefore overlap regions of bridging fibers due to Kif4A silencing.

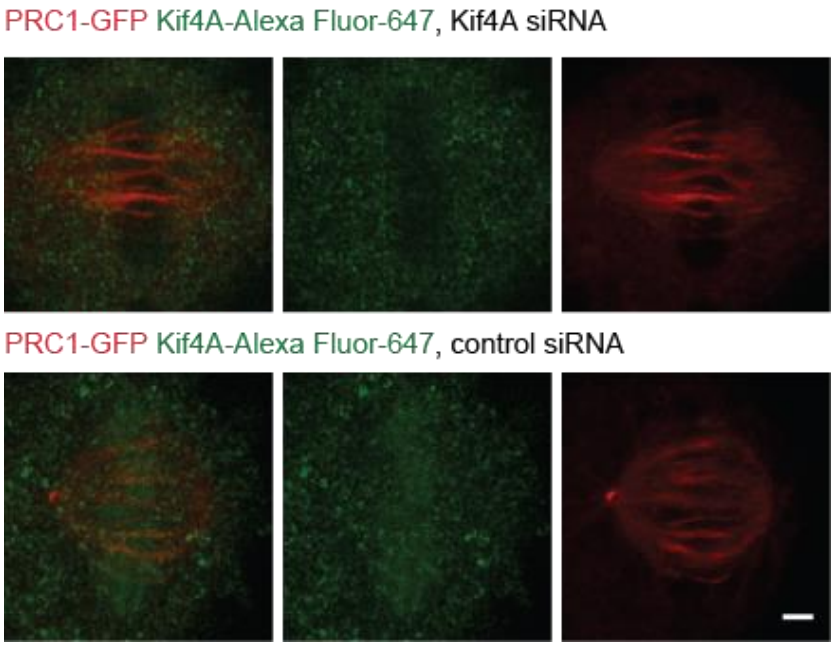

Figure 32. Kif4A silencing. HeLa cells stably expressing PRC1-GFP treated with siRNA targeting Kif4A (top images) and control siRNA (bottom images). One z-slice for each spindle is shown. Images are left: merge, middle: Alexa Flour-647, and right: GFP, respectively. Scale bar, 2 µm.

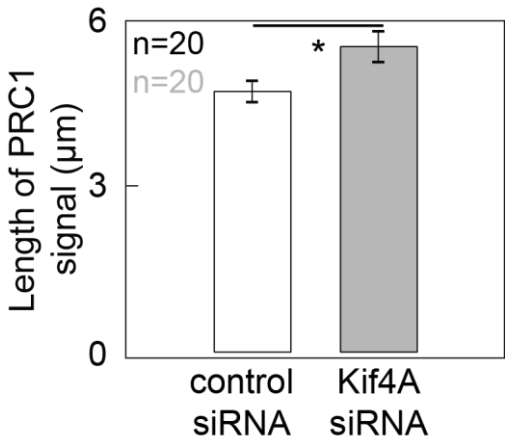

Figure 33. Kif4A silencing elongates bridging fiber. Comparison of the length between PRC1-GFP signals from HeLa cells stably expressing PRC1-GFP that are treated with control siRNA (white) and Kif4A siRNA (gray). P-value, 0.0212.

Contrary to previously reported results on Kif4A silencing causing unfocused overlap regions (Hu et al., 2011), measurements at the cross section of the bundles show statistically similar intensities. In control cell, intensity at the cross section of the bundle was 11.171 ± 1.264 a.u. (n=15 in 9 cells), whereas in cells treated with Kif4A siRNA was 10.018 ± 0.741 a.u. (n=24 in 8 cells). Together with this measurement, spindle length and width were analyzed in both control and Kif4A siRNA treated cells. Upon investigation, there was no apparent decrease or increase in these parameters. In control cells, spindle width was 8.705 ± 0.335 μm and length was 10.342 ± 0.327 μm (n=10 cells). In Kif4A siRNA treated cells, spindle width was 8.738 ± 0.200, whilst spindle length was 10.722 ± 0.386 (n=9 cells, p value for width was 0.450, p value for length was 0.4618). These data show that Kif4A silencing elongates overlap regions, while not affecting spindle length and width.

4. Discussion

I have shown that in metaphase, a kinesin-6 motor MKLP1 is associated with the spindle in its central part, where antiparallel regions are formed by interdigitating microtubules. By following pole-to-pole sister k-fiber curvatures, MKLP1 is found to be enriched in the gap between sister k-fibers and extend laterally from sister kinetochores. Length measurements of the MKLP1 signal have shown that MKLP1 extends over a region smaller than the previously reported length of PRC1-labeled bridging fibers (Kajtez et al., 2016, Polak et al., 2017). The length of the metaphase MKLP1-GFP signal calculated from pole-to-pole intensity profiles was 4.09 ± 0.15 µm (n=18 tracks from 9 cells), whereas it was shown that PRC1-labeled overlap regions of the bridging fibers are 4.5 ± 0.2 µm (Kajtez et al., 2016). This could be due to PRC1 being a passive cross-linker, whilst MKLP1 is a plus-end directed motor protein. However, MKLP1 signal was found to correlate with the signal of PRC1-labeled overlaps. Length of the MKLP1-GFP signal was 4.768 ± 0.183 µm and mCherry-PRC1 was 4.780 ± 0.187 µm (p=0.963, n=20 bundles in 7 cells), whereas thickness of the MKLP1-labeled bundle was 0.617 ± 0.02 µm and mCherry-PRC1 was 0.618 ± 0.02 µm (p=0.0996, n=15 bundles in 7 cells). Interestingly, the length of the MKLP1 signal was increased when PRC1 was overexpressed. Following PRC1 overexpression, MKLP1 was localized in all PRC1-labeled bundles. Since virtually all bridging fibers contain PRC1-labeled overlaps, MKLP1 is present within bridging fibers throughout the spindle. As proposed function of MKLP1 is to cross-link and slide antiparallel microtubules in the anaphase spindle (Nislow et al., 1992), MKLP1 bundles microtubules in the bridging fiber and generates forces within bridging fiber that would drive spindle elongation during anaphase B. Additionally, MKLP1 is a component of centralspindlin complex that has been implicated in the formation of the spindle midzone during mitosis (Zhu et al., 2005), therefore bridging fibers must have an important role in determination of the central spindle assembly.

Furthermore, Kif4A as a major binding partner of PRC1 was observed in the PRC1-labeled bundles in prometaphase. This could be due to relocalization of PRC1 toward the plus end of microtubules where overlap regions of bridging microtubules are formed. Consistent with previous findings that the spindle midzone and overlap regions elongate when Kif4A is depleted (Zhu and Jian, 2005; Bieling et al., 2010; Hu

et al., 2011), Kif4A silencing with Kif4A siRNA increased the length of PRC1-labeled bridging fibers in metaphase spindle since PRC1 is not properly translocated to the plus-ends of microtubules. In control cells, the length of PRC1-GFP signal was 4.714 ± 0.189 μm (n=20 in 9 cells). Yet, in cells treated with Kif4A siRNA, the length of PRC1-GFP signal was 5.527 ± 0.279 μm (p=0.021, n=20 in 8 cells). However, Kif4A depletion did not result in unfocused overlap regions of PRC1-labeled bridging fibers, contrary to Hu et al., 2011. In control cell, intensity at the cross section of the bundle was 11.171 ± 1.264 a.u. (n=15 in 9 cells), whereas in cells treated with Kif4A siRNA was 10.018 ± 0.741 a.u. (n=24 in 8 cells). Additionally, Kif4A silencing did not affect the length and the width of metaphase spindles. In control cells, spindle width was 8.705 ± 0.335 μm and length was 10.342 ± 0.327 μm (n=10 cells). In Kif4A siRNA treated cells, spindle width was 8.738 ± 0.200, whilst spindle length was 10.722 ± 0.386 (n=9 cells, p value for width was 0.450, p value for length was 0.4618). Thus, spindles undergo atypical elongation of PRC1-labeled bridging fibers when Kif4A is depleted without increasing the length and the width of the spindles.

Pole-to-pole tracking of Kif18A-GFP signal revealed that k-fibers located more than 3 μm away from the spindle long axis have Kif18A-GFP punctae at each sister kinetochore, while 70% of k-fibers located within 3 μm from the spindle long axis have only one Kif18A-GFP punctus positioned at one kinetochore (n=47 in 10 cells). Additionally, intensity of the outer Kif18-GFP punctae was 25.502 ± 2.16 a.u. (n=22 punctae in 10 cells), whereas intensity of inner punctae was 18.42 ± 2.213 a.u. (n=25 punctae in 10 cells). This is consistent with length-dependent effect of kinesin-8 in which longer microtubules, i.e. outer ones, lead to greater accumulation on their plus-end as the larger amount of kinesin-8 motors bind to them and move toward the plus-ends (Varga et al., 2006).

Among all inspected microtubule-based motors, I have shown that only MKLP1 localizes to central part of the metaphase spindle between sister kinetochores, where bridging fibers reside. Following the initiation of chromosome segregation, MCAK, Kif18A, Kif4A, and MKLP1 start to concentrate at the sites of microtubule plus-end overlaps. Interestingly, Eg5 accumulates at lateral parts of these central spindle bundles. As the aftermath of these translocations, motors generate the central spindle that later regulates cleavage furrow initiation and the completion of cytokinesis.

Due to PRC1 overexpression with mCherry-PRC1 plasmid, all kinesin motors have shown aberrant relocalization within the spindle and association with PRC1-labeled overlap regions. This change of localization could be a consequence of massive crosslinking of all neighboring fibers and therefore bundles of microtubules growing within them. In agreement with this, dynein motor DN1CH1 showed no atypical relocalization within the spindle. DN1CH1 as a minus-end directed motor retained its position at the spindle poles and the k-fibers. Thus, minus-ends of microtubules remained at the spindle poles and along k-fibers.

For future aspects, it will be important to examine the role of MKLP1 in the bridging fiber and to determine to which extent it contributes to the different phases of mitosis with respect to its position within the bridging fiber. Furthermore, it will be interesting to see if motors located at the k-fibers generate forces to slide chromosomes along the bridging fibers. Finally, it is necessary to understand why PRC1 overexpression prevents prometaphase-to-metaphase transition.

5. Conclusion

In this thesis, I have used confocal microscopy to show the localization of motor proteins with respect to positions of the bridging fibers. Upon investigation, MKLP1 was shown to be the most prominent candidate that localizes within the bridging fibers. MKLP1, a kinesin-6 motor, was observed in the central part of the spindle, spanning the region between sister kinetochores, where bridging fibers reside. Length of the MKLP1 signal was significantly less than the length of previously observed PRC1-labeled overlap regions of the bridging fibers. Overexpression of PRC1 with mCherry-PRC1 plasmid affected relocalization of kinesins within the mitotic spindle. These spindles with aberrant localization of motor proteins were unable to align chromosomes in the metaphase plate and therefore proceed from prometaphase to metaphase. Notably, overexpression of PRC1 in MKLP1-GFP cell line showed correlation between PRC1-labeled bundles and MKLP1 signal, both in length and intensity. Length of the MKLP1 signal, when PRC1 was overexpressed, was significantly increased, compared to untreated cells. Additionally, Kif4A, a kinesin-4 motor, which is major binding partner of PRC1, was shown to elongate PRC1-labeled overlaps of the bridging fibers when silenced. These elongated PRC1-labeled overlaps had similar intensity to PRC1-labeled overlaps in control cells.

6. Literature

Alberts B, Johnson A, Lewis J, Raff M, Roberts K, Walter P. Molecular biology of the cell. Garland Science, New York (2007).

Allan VJ. Cytoplasmic dynein. *Biochem Soc Trans*, **39**: 1169–1178 (2011).

Bakhoum SF, Genovese G, Compton DA. Deviant kinetochore microtubule dynamics underlie chromosomal instability. *Curr Biol*, **19**(22): 1937-1942 (2009).

Bieling P, Telley IA, Surrey T. A minimal midzone protein module controls formation and length of antiparallel microtubule overlaps. *Cell*, **142**(3): 420-432 (2010).

Bringmann H, Skiniotis G, Spilker A, Kandels-Lewis S, Vernos I, Surrey T. A kinesin-like motor inhibits microtubule dynamic instability. *Science*, **303**(5663): 1519-1522 (2004).

Cheeseman IM, Desai A. Molecular architecture of the kinetochore-microtubule interface. *Nat Rev Mol Cell Biol*, **9**: 33–46 (2008).

Cooper GM, Hausman RE. The cell: a molecular approach. Sinauer Associates, Sunderland (2003).

Desai A, Verma S, Mitchison TJ, Walczak CE. Kin I kinesins are microtubule-destabilizing enzymes. *Cell*, **96**: 69-78 (1999).

Ferenz NP, Paul R, Fagerstrom C, Mogilner A, Wadsworth P. Dynein antagonizes eg5 by crosslinking and sliding antiparallel microtubules. *Curr Biol*, **19**: 1833–1838 (2009).

Gable A, Qiu M, Titus J, Balchand S, Ferenz NP, Ma N, Collins ES, Fagerstrom C, Ross JL, Yang G, Wadsworth P. Dynamic reorganization of Eg5 in the mammalian spindle throughout mitosis requires dynein and TPX2. *Mol Biol Cell*, **23**(7): 1254-1266 (2012).

Gupta ML, Jr, Carvalho P, Roof DM, Pellman D. Plus end-specific depolymerase activity of Kip3, a kinesin-8 protein, explains its role in positioning the yeast mitotic spindle. *Nat Cell Biol*, **8**: 913–923 (2006).

Howard J, Hyman AA. Microtubule polymerases and depolymerases. *Curr Opin Cell Biol*, **19**(1): 31-35 (2007).

Howell BJ, McEwen BF, Canman JC, Hoffman DB, Farrar EM, Rieder CL, Salmon ED. Cytoplasmic dynein/dynactin drives kinetochore protein transport to the spindle

poles and has a role in mitotic spindle checkpoint inactivation. *J Cell Biol*, **155**(7): 1159–1172 (2001).

Hu CK, Coughlin M, Field CM, Mitchison TJ. KIF4 regulates midzone length during cytokinesis. *Curr Biol*, **21**(10): 815-824 (2011).

Jensen CG. Dynamics of spindle microtubule organization: kinetochore fiber microtubules of plant endosperm. *J Cell Biol*, **92**: 540-558 (1982).

Jiang W, Jimenez G, Wells NJ, Hope TJ, Wahl GM, Hunter T, Fukunaga R. PRC1: a human mitotic spindle-associated CDK substrate protein required for cytokinesis. *Mol Cell*, **2**: 877-885 (1998).

Kajtez J, Solomatina A, Novak M, Polak B, Vukušić K, Rüdiger J, Cojoc G, Milas A; Šumanovac Šestak I, Risteski P, Tavano F, Klemm AH, Roscioli E, Welburn J, Cimini D, Glunčić M, Pavin N, Tolić, IM. Overlap microtubules link sister k-fibres and balance the forces on bi-oriented kinetochores. *Nat Commun*, **7**: 10298 (2016).

Kapitein LC, Peterman EJ, Kwok BH, Kim JH, Kapoor TM, Schmidt CF. The bipolar mitotic kinesin Eg5 moves on both microtubules that it crosslinks. *Nature*, **435**(7038): 114-118 (2005).

Kapitein LC, Janson ME, van den Wildenberg SM, Hoogenraad CC, Schmidt CF, Peterman EJ. Microtubule-driven multimerization recruits ase1p onto overlapping microtubules. *Curr Biol*, **18**: 1713-1717 (2008).

Kapoor TM. Metaphase spindle assembly. *Biology*, **6**(1): 8 (2017).

Kashina AS, Baskin RJ, Cole DG, Wedaman KP, Saxton WM, Scholey JM. A bipolar kinesin. *Nature*, **379**(6562): 270–272 (1996).

Kim IG, Jun DY, Sohn U, Kim YH. Cloning and expression of human mitotic centromere-associated kinesin gene. *Biochim Biophys Acta*, **1359**(3): 181–186 (1998).

Kline-Smith SL, Khodjakov A, Hergert P, Walczak CE. Depletion of centromeric MCAK leads to chromosome congression and segregation defects due to improper kinetochore attachments. *Mol Biol Cell*, **15**(3): 1146–1159 (2004).

Kurasawa Y, Earnshaw WC, Mochizuki Y, Dohmae N, Todokoro K. Essential roles of KIF4 and its binding partner PRC1 in organized central spindle midzone formation. *EMBO J*, **23**: 3237-3248 (2004).

Le Guellec R, Paris J, Couturier A, Roghi C, Philippe M. Cloning by differential screening of a *Xenopus* cDNA that encodes a kinesin-related protein. *Mol Cell Biol*, **11**(6): 3395–3398 (1991).

Lee KY, Esmaeili B, Zealley B, Mishima M. Direct interaction between centralspindlin and PRC1 reinforces mechanical resilience of the central spindle. *Nat Commun*, **6**: 7290 (2015).

Maiato H, Sampaio P, Sunkel CE. Microtubule-associated proteins and their essential roles during mitosis. *Int Rev Cytol*, **241**: 53-153 (2004).

Maney T, Hunter AW, Wagenbach M, Wordeman L. Mitotic centromere-associated kinesin is important for anaphase chromosome segregation. *J Cell Biol*, **142**(3): 787-801 (1998).

Manning AL, Compton DA. Structural and regulatory roles of nonmotor spindle proteins. *Curr Opin Cell Biol*, **20**: 101 – 106 (2008).

Marchetti F, Massarotti A, Yauk CL, Pacchierotti F, Russo A. The adverse outcome pathway (AOP) for chemical binding to tubulin in oocytes leading to aneuploid offspring. *Environ Mol Mutagen*, **57**: 87-113 (2016).

Matuliene J, Kuriyama R. Kinesin-like protein CHO1 is required for the formation of midbody matrix and the completion of cytokinesis in mammalian cells. *Mol Biol Cell*, **13**(6): 1832-1845 (2002).

McDonald KL, O'Toole ET, Mastronarde DN. Kinetochore microtubules in PTK cells. *J Cell Biol*, **118**: 369-383 (1992).

McEwen BF, Chan GK, Zubrowski B, Savoian MS, Sauer MT, Yen TJ. CENP- E is essential for reliable bioriented spindle attachment, but chromosome alignment can be achieved via redundant mechanisms in mammalian cells. *Mol Biol Cell*, **9**: 2776-2789 (2001).

Merdes A, Ramyar K, Vechio JD, Cleveland DW. A complex of NuMA and cytoplasmic dynein is essential for mitotic spindle assembly. *Cell*, **87**(3): 447-58 (1996).

Merdes A, Heald R, Samejima K, Earnshaw WC, Cleveland DW. Formation of spindle poles by dynein/dynactin-dependent transport of NuMA. *J Cell Biol*, **149**(4): 851-862 (2000).

Milas A, Tolić, IM. Relaxation of interkinetochore tension after severing of a k-fiber depends on the length of the k-fiber stub. *Matters Select*, doi: 10.19185/ matters.201603000025 (2016).

Mishima M, Pavicic V, Grüneberg U, Nigg EA, Glotzer M. Cell cycle regulation of central spindle assembly. *Nature*, **430**(7002): 908-913 (2004).

Mitchison TJ, Maddox P, Gaetz J, Groen A, Shirasu M, Desai A, Salmon ED, Kapoor, TM. Roles of polymerization dynamics, opposed motors, and a tensile element in governing the length of *Xenopus* extract meiotic spindles. *Mol Biol Cell*, **16**: 3064–3076 (2005).

Mollinari C, Kleman JP, Jiang W, Schoehn G, Hunter T, Margolis RL. PRC1 is a microtubule binding and bundling protein essential to maintain the mitotic spindle midzone. *J Cell Biol*, **157**: 1175-1186 (2002).

Musacchio A, Desai A. A molecular view of kinetochore assembly and function. *Biology*, **6**(1): 5 (2017).

Mayr MI, Hummer S, Bormann J, Gruner T, Adio S, Woehlke G, Mayer TU. The human kinesin Kif18A is a motile microtubule depolymerase essential for chromosome congression. *Curr Biol*, **17**(6): 488-498 (2007).

Neef R, Gruneberg U, Kopajtich R, Li X, Nigg EA, Sillje H, Barr FA. Choice of Plk1 docking partners during mitosis and cytokinesis is controlled by the activation state of Cdk1. *Nat Cell Biol*, **9**: 436-444 (2007).

Nezi L, Musacchio A. Sister chromatid tension and the spindle assembly checkpoint. *Curr Opin Cell Biol*, **21**: 785–795 (2009).

Nislow C, Sellitto C, Kuriyama R, McIntosh JR. A monoclonal antibody to a mitotic microtubule-associated protein blocks mitotic progression. *J Cell Biol*, **111**(2): 511-522 (1990).

Nislow C, Lombillo VA, Kuriyama R, McIntosh JR. A plus-end-directed motor that moves anti-parallel microtubules in vitro localizes in the interzone of mitotic spindles. *Nature*, **359**: 543–547 (1992).

Nixon FM, Honnor TR, Clarke NI, Georgina P, Beckett AJ, Johansen AM, Brettschneider JA, Prior A, Royle SJ. Microtubule organization within mitotic spindles revealed by serial block face scanning EM and image analysis. *J Cell Sci*, **130**: 1845-1855 (2017).

Ogawa T, Nitta R, Okada Y, Hirokawa N. A common mechanism for microtubule destabilizers-M type kinesins stabilize curling of the protofilament using the class-specific neck and loops. *Cell*, **116**: 591-602 (2004).

Ohi R, Coughlin ML, Lane WS, Mitchison TJ. An inner centromere protein that stimulates the microtubule depolymerizing activity of a KinI kinesin, *Dev Cell*, **5**: 309-321 (2003).

Pavin N, Tolić IM. Self-organization and forces in the mitotic spindle. *Annu Rev Biophys*, **45**: 279–98 (2016).

Pellman D, Bagget M, Tu YH, Fink GR, Tu H. Two microtubule-associated proteins required for anaphase spindle movement in *Saccharomyces cerevisiae*. *J Cell Biol*, **130**: 1373-1385 (1995).

Polak B, Risteski P, Lesjak S, Tolić IM. PRC1-labeled microtubule bundles and kinetochore pairs show one-to-one association in metaphase. *EMBO Rep*, **18**: 217-230 (2017).

Poser I, Sarov M, Hutchins JR, Heriche JK, Toyoda Y, Pozniakovsky A, Weigl D, Nitzsche A, Hegemann B, Bird AW et al. BAC TransgeneOmics: a high- throughput method for exploration of protein function in mammals. *Nat Methods*, **5**: 409–415 (2008).

Radulescu AE, Cleveland DW. NuMA after 30 years: the matrix revisited. *Trends Cell Biol*, **20**(4): 214–222 (2010).

Rusan NM, Tulu US, Fagerstrom C, Wadsworth P. Reorganization of the microtubule array in prophase/prometaphase requires cytoplasmic dynein-dependent microtubule transport. *J Cell Biol*, **158**(6): 997-1003 (2002).

Sawin KE, LeGuellec K, Philippe M, Mitchison TJ. Mitotic spindle organization by a plus-end directed microtubule motor. *Nature*, **359**: 540–543 (1992).

Scholey JM, Civelekoglu-Scholey G, Brust-Mascher I. Anaphase B. *Biology*, **5**(4): 51 (2016).

Sharp DJ, Rogers GC, Scholey JM. Cytoplasmic dynein is required for poleward chromosome movement during mitosis in *Drosophila* embryos. *Nat Cell Biol*, **2**: 922–930 (2000).

Shimamoto Y, Forth S, Kapoor TM. Measuring pushing and braking forces generated by ensembles of kinesin-5 crosslinking two microtubules. *Dev Cell*, **34**(6): 669-681 (2015).

Simunić J, Tolić IM. Mitotic Spindle assembly: building the bridge between sister k-fibers. *Trends Biochem Sci,* **41**(10): 824-833 (2016).

Subramanian R, Wilson-Kubalek EM, Arthur CP, Bick MJ, Campbell EA, Darst SA, Milligan RA, Kapoor TM. Insights into antiparallel microtubule crosslinking by PRC1, a conserved nonmotor microtubule binding protein. *Cell*, **142**: 433-443 (2010).

Stumpff J, von Dassow G, Wagenbach M, Asbury C, Wordeman L. The kinesin-8 motor Kif18A suppresses kinetochore movements to control mitotic chromosome alignment. Dev Cell, **14**: 252–262 (2008).

Su X, Arellano-Santoyo H, Portran D, Gaillard J, Vantard M, Thery M, Pellman D. Microtubule sliding activity of a kinesin-8 promotes spindle assembly and spindle length control. *Nat Cell Biol*, **15**(8): 948–957 (2013).

Subramanian R, Ti SC, Tan L, Darst SA, Kapoor TM. Marking and measuring single microtubules by PRC1 and kinesin-4. *Cell*, **154**: 377-390 (2013).

Tanenbaum ME, Macůrek L, Galjart N, Medema RH. Dynein, Lis1 and CLIP-170 counteract Eg5-dependent centrosome separation during bipolar spindle assembly. *EMBO J*, **27**: 3235–3245 (2008).

Tanenbaum ME, Akhmanova A, Medema RH. Dynein at the nuclear envelope. *EMBO Rep*, **11**: 649 (2010).

Tanenbaum ME, Medema RH, Akhmanova A. Regulation of localization and activity of the microtubule depolymerase MCAK. *Bioarchitecture*, **1**(2): 80-87 (2011).

Tanenbaum ME, Vale RD, McKenney RJ. Cytoplasmic dynein crosslinks and slides anti-parallel microtubules using its two motor domains. *eLife*, **2**: e00943 (2013).

Tolić IM, Pavin N. Bridging the gap between sister kinetochores. *Cell Cycle*, **15**: 1169–1170 (2016).

Tolić, IM. Mitotic spindle: kinetochore fbers hold on tight to interpolar bundles. *Eur Biophys J*, doi: 10.1007/s00249-017-1244-4 (2017).

van Beuningen SF, Will L, Harterink M, Chazeau A, van Battum EY, Frias CP, Franker MA, Katrukha EA, Stucchi R, Vocking K, Antunes AT, Slenders L, Doulkeridou S, Sillevis Smitt P, Altelaar AF, Post JA, Akhmanova A, Pasterkamp RJ, Kapitein LC, de Graaff E, Hoogenraad CC. TRIM46 controls neuronal polarity and axon specification by driving the formation of parallel microtubule arrays. *Neuron*, **88**(6): 1208-1226 (2015).

Varga V, Helenius J, Tanaka K, Hyman AA, Tanaka TU, Howard J. Yeast kinesin-8 depolymerizes microtubules in a length-dependent manner. *Nat Cell Biol*, **8**: 957–962 (2006).

Walczak CE, Mitchison TJ, Desai A. XKCM1: a *Xenopus* kinesin-related protein that regulates microtubule dynamics during mitotic spindle assembly. *Cell*, **84**(1): 37-47 (1996).

Wang SZ, Adler R. Chromokinesin: a DNA-binding, kinesin-like nuclear protein. *J Cell Biol*, **128**(5): 761-768 (1995)

Waters JC, Salmon ED. Pathways of spindle assembly. *Curr Opin Cell Biol*, **9**: 37–43 (1997).

Wendell KL, Wilson L, Jordan MA. Mitotic block in HeLa cells by vinblastine: ultrastructural changes in kinetochore-microtubule attachment and in centrosomes. *J Cell Sci*, **104**: 261-274 (1993).

Wojcik EJ, Buckley RS, Richard J, Liu L, Huckaba TM, Kim S. Kinesin-5: cross-bridging mechanism to targeted clinical therapy. *Gene*, **531**(2): 133–149 (2013).

Wordeman L, Mitchison TJ. Identification and partial characterization of mitotic centromere-associated kinesin, a kinesin-related protein that associates with centromeres during mitosis. *J Cell Biol*, **128**(1-2): 95-104 (1995).

Wordeman L. Microtubule-depolymerizing kinesins. *Curr Opin Cell Biol*, **17**(1): 82-88 (2005).

Zhu C, Bossy-Wetzel E, Jiang W. Recruitment of MKLP1 to the spindle midzone/midbody by INCENP is essential for midbody formation and completion of cytokinesis in human cells. *Biochem J*, **389**(2): 373-381 (2005).

Zhu C, Zhao J, Bibikova M, Leverson JD, Bossy-Wetzel E, Fan JB, Abraham RT, Jiang W. Functional analysis of human microtubule-based motor proteins, the kinesins and dyneins, in mitosis/cytokinesis using RNA interference. *Mol Biol Cell*, **16**(7): 3187-3199 (2005).

Zhu C, Jiang W. Cell cycle-dependent translocation of PRC1 on the spindle by Kif4 is essential for midzone formation and cytokinesis. *Proc Natl Acad Sci USA*, **102**(2): 343-348 (2005).

Zhu C, Lau E, Schwarzenbacher R, Bossy-Wetzel E, Jiang W. Spatiotemporal control of spindle midzone formation by PRC1 in human cells. *Proc Natl Acad Sci USA*, **103**(16): 6196-6201 (2006).

7. Curriculum vitae

Personal information

Patrik Risteski

14 November 1991

Pula, Croatia

Education

Undergraduate program in Molecular Biology, Department of Biology, Faculty of Science, University of Zagreb, Zagreb (Croatia)

Mathematical Gymnasium Pula, Pula (Croatia)

Publications

Polak B*, Risteski P*, Lesjak S, Tolić IM. PRC1-labeled microtubule bundles and kinetochore pairs show one-to-one association in metaphase. *EMBO Rep*, 18(2): 217–230 (2017).

Kajtez J*, Solomatina A*, Novak M*, Polak B, Vukušić K, Rüdiger J, Cojoc G, Milas A; Šumanovac Šestak I, Risteski P, Tavano F, Klemm AH, Roscioli E, Welburn J, Cimini D, Glunčić M, Pavin N, Tolić IM. Overlap microtubules link sister k-fibres and balance the forces on bi-oriented kinetochores. *Nat Commun*, 7: 10298 (2016).

*equal contribution

Conferences

Risteski P, Vukušić K, Buđa R, Bosilj A, Milas A, Pavin N, Tolić IM. Microtubule sliding in the bridging fiber pushes kinetochore fibers apart to segregate chromosomes in human cells. ASCB | EMBO Meeting 2017, Philadelphia (PA, United States), oral and poster presentation.

Polak B, Risteski P, Simunić J, Lesjak S, Tolić IM. One-to-one association between PRC1-labeled microtubule bundles and kinetochore pairs in metaphase. EMBO | EMBL Symposium: Microtubules: From Atoms to Complex Systems 2016, Heidelberg (Germany), poster presentation.

Kajtez J, Solomatina A, Risteski P, Novak M, Polak B, Vukušić K, Milas A, Pavin N, Tolić IM. Overlap microtubules link sister k-fibres and balance the forces on bi-oriented kinetochores. EMBO Meeting 2015, Birmingham (United Kingdom), oral and poster presentation.

Workshops

Polak B, Risteski P, Simunić J, Lesjak S, Tolić IM. One-to-one association between PRC1-labeled microtubule bundles and kinetochore pairs in metaphase. Dynamics of the Cytoskeleton 2016, Zagreb (Croatia), poster presentation.

Awards

Rector's Acknowledgement for International Scientific Achievements 2017, Zagreb (Croatia)

Scholarship for Excellent Students of Istria County 2015-2017, Pula (Croatia)

ASCB International Travel Award for ASCB | EMBO Meeting 2017, Philadelphia (PA, United States)

EMBO Travel Grant for EMBO Meeting 2015, Birmingham (United Kingdom)

Courses

Greta Pifat Mrzljak International School of Biophysics 2014, Primošten (Croatia)

Science popularization

Open Day of the Institute 2017, Ruđer Bošković Institute, Zagreb (Croatia)

Open Day of the Institute 2016, Ruđer Bošković Institute, Zagreb (Croatia)

Night of Biology 2014, Faculty of Science, University of Zagreb, Zagreb (Croatia)

“Somewhere, something incredible is waiting to be known.”

- Carl Sagan